NASA Technical Memorandum 84640

Halogen Occultation Experiment (HALOE) Gas Cell Life Test Program

Edward M. Sullivan, Robert E. Thompson,
Gale A. Harvey, Jae H. Park,
and D. J. Richardson

AUGUST 1983

25th Anniversary
1958-1983

NASA

NASA Technical Memorandum 84640

Halogen Occultation Experiment (HALOE) Gas Cell Life Test Program

Edward M. Sullivan
Langley Research Center
Hampton, Virginia

Robert E. Thompson
Systems and Applied Sciences Corporation
Hampton, Virginia

Gale A. Harvey and Jae H. Park
Langley Research Center
Hampton, Virginia

D. J. Richardson
Systems and Applied Sciences Corporation
Hampton, Virginia

National Aeronautics
and Space Administration

**Scientific and Technical
Information Branch**

1983

CONTENTS

SUMMARY

The Halogen Occultation Experiment (HALOE) will use gas filter correlation radiometry to measure the atmospheric concentration profiles of HCl, HF, NO, and CH_4 from the Upper Atmosphere Research Satellite. Because the containment of these gases in gas filter cells for an extended period (several years) of time is essential to the success of HALOE, a gas cell life test program has been undertaken to support the HALOE instrument development at Langley Research Center. The primary objectives of this test program are to demonstrate the integrity of the cells and the concentration stability of the gases in the cells by exposing filled cells to simulated storage and flight environments. A secondary objective is to identify the sources of contaminants in the contained gases so that the possibility of preventing their appearance in the HALOE instrument cells can be explored.

The life test program consists of three types of tests: long-term storage, accelerated aging, and thermal cycling. In addition, thermal effects tests are conducted to provide information which may be required for HALOE data interpretation. Each test utilizes its own special apparatus. The primary data are infrared spectra from the gases in the cells. These spectra are obtained with a Fourier Transform Infrared Interferometer and analyzed with a nonlinear least-squares fitting technique developed specifically for this program. The analysis uses the best available spectral data to fit a number of lines from the measured spectra and calculate the pressure, optical mass, and mixing ratio of the gases in the cells. The available data show that none of the gas cells in the life test program has leaked even though some of these cells have been filled for over 2 years, and several of them have been exposed to one or more of the tests mentioned. Two of the cells which contain HF at very low pressure and mixing ratio have shown a decrease in the HF concentration with time, but since there is no corresponding detectable increase in the total pressure, this is believed to be caused by wall sorption effects and chemical reactions and not by a leak. All the cells which contain HF show changes in interior appearance. These changes are being monitored but since there are no leaks involved the cells are proceeding through the life test program in the prescribed fashion.

1 INTRODUCTION

1.1 Purpose of HALOE

The Halogen Occultation Experiment (HALOE) is a satellite experiment to measure, on a global basis, the concentration profiles of a number of trace constituents in the stratosphere (ref. 1). The species to be measured are: O_3, HCl, HF, NO, CH_4, H_2O, and NO_2. (In order to correlate the data as a function of atmospheric pressure, the CO_2 transmittance profile is also measured.) These species were selected because they will permit the scientific community to study stratospheric ozone depletion resulting from chlorine in the stratosphere and to determine the relative amounts of chlorine from natural and man-made sources. Stratospheric ozone is vital to terrestrial life because it filters out much of the harmful solar ultraviolet radiation. Thus, the possibility of ozone depletion resulting from man-made chemical compounds entering the atmosphere has been a major concern for the past two decades (e.g., refs. 2 to 5). The concern over the particular effects of chlorine released from man-made chemical compounds (especially the fluorocarbons $CFCl_3$ and CF_2Cl_2) used

as refrigerants, cleaning compounds, and foaming agents has surfaced more recently (refs. 6 and 7). It is this latter concern that HALOE will address directly. The data derived from HALOE will, however, permit extensive studies of stratospheric chemistry as a whole and in particular will permit studies of the interactions between the oxides of nitrogen (NO_x), chlorine (ClO_x), hydrogen (HO_x), and their overall effect on stratospheric ozone.

1.2 HALOE Measurement Technique

The HALOE instrument measures the atmospheric absorption of solar radiation in the spectral range from 2 to 10 μm during both sunrise and sunset occultation events. By measuring the solar radiation with and without the intervening atmosphere during a solar occultation, the absorption of the solar infrared by the atmosphere can be determined and the concentration of the specified atmospheric trace species can be calculated. The instrument uses both conventional optical filter radiometers (O_3, H_2O, NO_2, and CO_2) and gas filter correlation radiometers (HCl, HF, CH_4, and NO). Conventional optical filters have a long history of application and are not discussed further in this report.

Gas filters can be used where a high degree of specificity is required. In the gas filter concept, a specified quantity of the gas of interest, at a known pressure and temperature, is placed in a correlation cell in the optical path of the instrument. The correlation of the spectral content of the atmospheric signal and the spectral signature of the gas in the cell provides a signal which can be interpreted in terms of the atmospheric concentration of the filtering gas (ref. 1).

1.3 Need for Gas Cell Life Test Program

The application of a gas filter approach to satellite applications is relatively new. The technique was pioneered at the University of Oxford by the application of the Selective Chopper Radiometer (SCR) and the Pressure Modulation Radiometer (PMR) on the Nimbus satellites. The technique was also employed by the Langley Research Center for the Measurement of Air Pollution from Satellites (MAPS) experiment which measured global tropospheric carbon monoxide during the second Space Shuttle mission. The PMR, MAPS, and HALOE approaches differ in that the PMR instrument modulates the pressure of the gas in the filter cell, whereas in MAPS and HALOE, the total pressure of the gas in the filter cell is fixed and fluctuates over a narrow range because of natural temperature variations. The PMR and MAPS measurement approaches both differ from HALOE in that PMR and MAPS are nadir-viewing instruments, whereas HALOE takes data during solar occultations.

The key to the success of the gas filter measurement technique is the ability to contain specific quantities of the gases of interest at known pressure and temperature in the instrument for several years. The HALOE design calls for the four gases of interest (HCl, HF, CH_4, and NO) to be contained in sealed cylindrical cells. The windows on either end of each cell are made from optical grade sapphire (Al_2O_3) which readily transmits the infrared spectral wavelengths of interest. The cell walls are made of either borosilicate glass (for the NO and CH_4 cells) or high purity gold (for the HCl and HF cells). These materials were selected because preliminary studies indicated they could withstand the handling, storage, and launch environments of the instrument and, for HCl and HF, the corrosive properties of the gases contained. The life test program described in this report was planned to prove that the materials

selected, and the cell fabrication techniques being used were suitable for HALOE. Other objectives of this life test program are to insure that

1. Any problems of fill gas/cell material chemical interaction have been solved

2. Fill gas concentration is not affected by the thermal and vacuum environments to be encountered in space

3. The sources of contaminants in the fill gases are found, and the possibility of preventing their appearance in the HALOE instrument cells is explored

The integrity of the gas cells under launch environment was demonstrated prior to the initiation of the life test program by subjecting one glass cell and one gold cell to the appropriate launch load conditions. This environmental test was not part of the life test program. The possibility exists, however, that extended storage of filled flight cells can result in minor corrosion or thermal stress effects with resultant failures during exposure to the launch environment. The HALOE schedule includes plans to expose one life test gold cell and one glass cell to simulated launch shock and vibration environments at some future time.

2 GAS CELL DESCRIPTION

The HALOE instrument contains two types of gas cells: correlation cells and calibration cells. Each type of cell is further grouped into two kinds: glass cells and gold cells. The correlation cells are 10 cm (4 in.) long and 2.5 cm (1 in.) in diameter. The calibration cells are 2.5 cm long and 2.5 cm in diameter. Since the materials and fabrication techniques are identical for both types of cells, the calibration cells were excluded from the life test program. The program does, however, include four gold correlation cells filled to pressures and mixing ratios which approximate the calibration cell fill conditions for HF and HCl. The fill conditions for these cells were chosen to meet two objectives: monitor the stability of the gases at low pressures and mixing ratios, and provide cells for use during the HALOE instrument test program.

The cell dimensions are a compromise between the practical aspects of the instrument design, viz minimizing volume and weight, and the science requirement that the cell contain a desired optical mass. A further consideration is that the optical mass and the pressure of the gas in the cell are small enough to avoid interference by other gases but large enough to overcome the Doppler shift of absorption lines caused by the relative motion between the satellite and the Sun.

2.1 Glass Gas Cell Fabrication

The glass gas cell design is the same as that used for the MAPS experiment. These cells are fabricated from cylinders of borosilicate glass with the sapphire windows fused to each end. The cells are filled through two tubes built into the glass cylinder. When the cell fill process is complete, the fill tubes are heated and fused to give a permanent seal. Figure 1 is a dimensioned drawing of the glass correlation cells and figure 2 is a photograph of a completed glass correlation cell used in the life test program.

2.2 Gold Gas Cell Fabrication

The fabrication technique for the gold cells is basically a gold electroform process. A hollow copper mandrel is prepared with an outside diameter equal to the desired inside diameter of the gas cell. A very thin (<1 μm) coat of gold is then vapor deposited over the body of the mandrel with the ends masked off. The periphery of each sapphire window is sputtered with a thin coat (250 Å) of chrome followed by a thicker (2500 Å) layer of gold. The chrome layer is necessary because gold does not readily adhere to the sapphire window. The windows are epoxied into place on the mandrel and the entire assembly is immersed in a gold plating bath until the gold has grown to the prescribed thickness (0.05 cm) and has made a secure joint at the window-body interface. The copper is etched out through the fill tubes with an acid solution. The epoxy residue is also washed out with a strong cleaning agent. Finally, the cell is rinsed with deionized water. The etching and cleaning processes are repeated until tests of the cleaning solution show residual copper to be <0.01 mg/L. The cell is helium leak checked to 10^{-10} cm^3/sec and then filled to the prescribed pressure and mixing ratio. At the end of the filling process, the fill tubes are pinched off to form a seal. Figure 3 is a dimensioned drawing of the gold cells and figure 4 is a photograph of a completed gold cell used in the life test program.

2.3 Gas Cell Fill

The fill conditions for each cell were specified based on an analysis of the length, weight, internal pressure, and optical mass compromises previously described. In most cases, the optical mass and pressure conditions for the cells as specified by HALOE science requirements dictated that the primary gas be diluted so that the mixing ratio would be <1.0. In these cases, the diluent was dry nitrogen. After each cell was fabricated, it was filled in a dedicated fill station. The fill procedures provided for passivation (i.e., allow a chemical reaction to occur until one of the reactants is depleted) of the cell walls, mixing of the gas with N_2 to achieve the correct mixing ratio, and sealing of the cell as described in the previous sections.

3 GAS CELL LIFE TEST PROGRAM PLAN

3.1 Program Plan Considerations

The HALOE gas cell life test program was designed to meet the objectives given in section 1.3. From these it became apparent that the output from the test program would be a determination of the concentration and pressure stability of the gases in the cells. This stability can be affected by leaks (cell integrity), by chemical reactions between the gases and the cell materials, and by adsorption or absorption of the gases by the cell walls. Chemical reactions and sorption processes (and the ability to detect them) can be influenced by time, temperature, gas pressure, and gas concentration (mixing ratio).

3.2 Test Program Elements

The life test program plan being followed is presented in table 1. As this chart shows, a set of either four or five cells is dedicated to each of the gases of interest. Each cell has been assigned one or more of the tests planned: long-term storage at room temperature, accelerated aging, and thermal cycling. It should be

noted that these cells are life test cells and will not be used in the HALOE instrument. New cells, designated as flight cells will be used for that purpose.

3.2.1 Long-term storage.- The long-term storage tests consist of maintaining the selected cells in a specified environment for the duration of the test. As shown in table 1, two environments have been specified: room temperature and pressure and room temperature and vacuum. The room temperature and pressure storage test recognizes that the flight cells will be exposed to atmospheric conditions from the time they are filled until the HALOE instrument is launched. The vacuum storage test is included because, after launch, the cells will be exposed to the space vacuum environment. In the atmospheric pressure environment, since the cells are filled to less than atmospheric pressure, the cells are subjected to a compressive stress regime. In the space vacuum environment, the external pressure will fall to a very low value and the wall tensile stresses caused by the internal pressure will dominate. It was deemed important to study this effect even though the pressure gradients available from a laboratory vacuum system will not approach the pressure gradients in the space environment. The HALOE launch is now scheduled for late 1989 (as compared with the original launch date of 1984) so that at launch the flight cells will be 6 to 8 years old. The life test cells will be maintained and monitored on a regular basis through 1987 to insure that the concentration of the fill gas in each cell remains stable for the required number of years.

3.2.2 Accelerated aging.- At least two cells in each group are to be exposed to an accelerated aging test in which the cells are exposed to an elevated temperature for a period of time (test A, table 1). This test is based on the empirical rule: "The rate at which chemical reactions occur will double for each 10°C increase in temperature." Stated differently, the rule says that the length of time required for a reaction to proceed to a given state will be halved if the temperature is raised 10°C. The factor of 1/2 cannot be verified for this application, but the accelerated aging tests can be used to establish quickly whether chemical reactions will occur in the gas cells. These tests also provide cells with a "chemical age" which is greater than their actual calendar age. These cells should be the first to show any indications of gas concentration changes due to chemical reactions or leakage due to chemically induced corrosion or cracking.

For the accelerated aging tests, a temperature of 85°C was chosen with a time of 400 hours. The room temperature is near 25°C so that the temperature difference is 60°C. The empirical rule then gives the "chemical age" as 400×2^6 hours or approximately 3 years as contrasted to the calendar age of 400 hours or 0.05 year.

3.2.3 Thermal cycling.- In the thermal cycling test (test C, table 1), the cells are cycled between specified temperature limits for a given number of cycles. Thermal design studies of the HALOE instrument have shown possible temperature extremes of -12°C to +23°C with smaller cyclic variations during each orbit. That is, the maximum temperature fluctuation of the HALOE instrument is 35°C over a period of 6 months and up to four such cycles over the experiment lifetime. During this time the HALOE instrument will experience approximately 8600 smaller ($\approx \pm 2$°C) temperature fluctuations. These combined temperature fluctuations will induce thermal stresses in the gas cells which could cause cell failure. The cyclic life test parameters were chosen as 2000 cycles between temperature limits of approximately 7°C to 37°C (ΔT = 30°C) with a cycle time of 30 minutes. This is a severe test since the induced thermal stresses approach the maximum stress level to be encountered by the cells in the instrument, the number of times the stress levels are encountered is at least

500 times greater than the number of times the flight cells will encounter comparable stress levels, and the cycle time is much shorter than the equivalent cycle time in orbit.

3.2.4 Thermal effects tests.- In addition to the tests just described which constitute the major elements of the gas cell life test program, two other tests, basically for gas cell research, are to be conducted once on at least one life test cell from each group (test D, table 1). The first of these tests is a depressed temperature test in which the cells are taken to -15°C, which is lower than the temperature that the flight cells will experience in the HALOE instrument while mounted in the Fourier Transform Infrared (FTIR) Interferometer described in section 4.1. This test investigates the influence of temperature on the adsorption or absorption of gases by the cell wall. The test also provides reference values for the spectral characteristics of the cell transmittance at the lowest temperatures that HALOE will encounter during the mission. The second test is the elevated temperature (50°C) version of the low temperature test. The effects of desorption by the cell walls are studied, and reference values for the spectral characteristics of the cell transmittance data at the highest temperatures that HALOE will encounter are obtained.

4 GAS CELL LIFE TEST IMPLEMENTATION

The gas cell life test program is being implemented in a dedicated laboratory at the Langley Research Center. The gas cells and all test equipment are kept in this room which is maintained at a temperature of 22°C ± 1°C and a relative humidity of 45 percent ± 10 percent.

4.1 Fourier Transform Spectroscopy

Measurement of the gas concentration in the life test cells is done by quantitative infrared absorption spectroscopy. A Fourier Transform Infrared Interferometer with a nominal resolution (as defined by the maximum displacement of the moving mirror in the interferometer) of approximately 0.06 cm^{-1} is used to obtain absorption spectra of the gases contained in the cells. These spectra are analyzed with the procedure described in section 5 to obtain the optical mass, pressure, and mixing ratio of the gases in the cells.

The measured spectral lines used in the analysis program have widths from approximately 0.001 to 0.1 cm^{-1}. Analyses of these spectra to retrieve the pressure and optical mass of the gases in the cells to the desired level of accuracy require that the spectra be of very high resolution with very low noise. These requirements dictate that the interferometer be very stable; this is accomplished by maintaining the room temperature and humidity within the narrow limits noted previously. The temperature of the interferometer optical bed is maintained at 28.5°C ± 0.3°C to minimize misalignment effects during data-taking periods.

Humidity inside the optical bed hood is maintained at a very low, almost constant level. This contributes to instrument stability and also minimizes the effects which water vapor in the interferometer optical path might have on the data. The humidity is controlled by sealing the hood to minimize the transport of room air into the space immediately over the optical bench, by constantly purging the hood with dry nitrogen obtained from the boiloff of a pressurized liquid nitrogen dewar, and by using dry nitrogen from this same dewar to provide the pressurized gas required for

the gas bearings on which the interferometer moving mirror rides. The humidity can be further controlled by means of a refrigerated cold trap mounted inside the hood.

The interferometer operating conditions which provide the best spectral data for the gas cell life test program were determined by experimentation over an extended period of time. The optimum gas bearing pressure has been established so that optical noise introduced by jitter or misalignment of the moving mirror is a minimum. The optical and electronic filters were selected to minimize the noise in the spectra for each gas of interest. The interferometer alignment techniques were developed so that alignment is maintained for many months. Interferogram data averaging was studied and it was determined that spectra obtained from 32 interferometer scans provided the best compromise between accuracy and operating time. As a result of all these investigations, the interferometer routinely provides the gas cell life test program with spectra which yield 0.2 percent to 0.3 percent rms noise in transmittance.

4.2 Life Test Equipment and Procedures

4.2.1 Long-term storage.- All gas cells in the life test program are stored at ambient temperature in the HALOE laboratory at the Langley Research Center. The cells stored under vacuum conditions are kept in dry-seal glass dessicator vessels at pressures of approximately 200 μm. The vacuum seal is normally broken only to remove cells so that data can be taken with the interferometer. After the spectral data are obtained, the cells are returned to the dessicator vessel and the vacuum reestablished.

4.2.2 Accelerated aging.- The cells selected for accelerated aging are removed from their normal long-term storage and mounted in a special aluminum cradle. This cradle has fluid-carrying heat-transfer lines machined into it which are connected by flexible hoses to a temperature controlled circulator with water as the working fluid. A single thermocouple is taped to the midpoint of the cell wall, and the cradle and cell are placed in a styrofoam container which thermally insulates them from the laboratory temperature. The temperature of the circulator is controlled so as to maintain the cell temperature, as determined by the thermocouple, to 85°C ± 0.1°C. These conditions are maintained for the 400 hours of the accelerated aging test. If spectral data for the cell are desired during this test period, it is necessary to remove the cell from the test cradle so that it can be placed in the interferometer. When this occurs, the time for the accelerated aging test is the sum of those time increments when the cell is at 85°C. The temperature history of the cell is maintained by manually noting times in a test log book.

4.2.3 Thermal cycling.- The cells selected for the thermal cycling tests are wrapped with 16 turns of 0.025-cm resistance heating wire which is connected to the secondary of a variable ac transformer. As current is passed through the resistance heating wire, the cell is heated and temperature control is achieved by controlling the current passed by the transformer. The cell is also wrapped with 1-cm (o.d.) surgical tubing connected to a refrigerated cooling circulator which uses ethylene glycol as a working fluid. When cooled fluid flows through the tubing, the cell is cooled and temperature control is achieved by controlling the circulator.

The current from the transformer and the fluid flow from the circulator are controlled by a programmed electronic timer. This timer has been set for a period of 30 minutes: 20 minutes heating, 2 minutes off and 7 minutes cooling, 1 minute off. This provides the desired cyclic temperature range. Cell temperatures are monitored

by means of two thermocouples taped to the cell wall approximately 2.5 cm from one end of the cell. One thermocouple is connected to a digital continuously displaying readout so that the temperature can be monitored at any time. The other thermocouple is connected to a strip chart recorder so that a permanent record of the number of cycles and temperature history is obtained.

4.2.4 Thermal effects tests.- The cells selected for investigation of temperature effects on the spectroscopic characteristics of the gases in the cells are wrapped with 6-mm (o.d.) surgical tubing. This tubing is connected to a controlled temperature circulator. The cell temperature is monitored by a thermocouple taped to the cell wall. The cell is installed in a special mounting cradle which thermally insulates the cell from the mounting cradle. Both cell and cradle are placed in the sample compartment of the FTIR and the circulator temperature adjusted until the cell temperature has stabilized at the desired value to within ±0.2°C. The FTIR interferometer scanning procedures are initiated and the cell spectral data are obtained.

5 FOURIER TRANSFORM SPECTRAL ANALYSIS METHOD

In order to meet the HALOE science requirements the gas cell total pressure and mixing ratio must be known to within ±5 percent. The cells must be filled to within approximately ±10 percent of the specified pressure and mixing ratio conditions and these conditions must not change by more than ±3 percent for the cells containing CH_4 and HCl, ±5 percent for the cells containing NO, and ±10 percent for the cells containing HF. These stability values apply over the lifetime of the cells, which is 4 years or more. The method used to analyze the interferometer data provides the capability of determining both the fill conditions and the gas concentration stability to the desired accuracies.

5.1 Spectral Data Analysis

The spectral data obtained from the interferometer are analyzed with a nonlinear least-squares technique (ref. 8). This technique is based on the Levenberg-Marquardt algorithm (ref. 9) and the nonlinear least-squares technique of Chang and Shaw (ref. 10). The technique solves a system of nonlinear equations of the functional form $f_i(x_j) = 0$ where $i = 1, 2, \ldots, N$, $j = 1, 2, \ldots, M$. The equations being solved are

$$f_i(x_j) = \frac{B_i}{B_{b_i}} - I_{o_i} \bar{\tau}_i(x_j) \qquad (1)$$

where

N number of sample data points, i

M number of independent variables, j

x_j independent parameters, viz total pressure, optical mass, instrument line shape function, fitted background of observed spectrum, and absorption line position

B_i observed radiance incident on interferometer detector with gas cell in place (single beam spectrum)

B_{b_i} observed radiance incident on interferometer detector with evacuated gas cell in place (single beam spectrum)

I_{o_i} fitted background of spectrum

$\bar{\tau}_i$ calculated transmittance; a function of p_t and U convolved with instrument line shape function

The calculation procedure requires that the transmittance, the fitted background of the spectrum, and the instrument line shape function be modeled. First, the optical mass is determined from a series of weakly absorbing (pressure independent) lines. The resulting optical mass is used in the calculation of the pressure from a series of strongly absorbing lines. Iteration procedures are used to adjust the calculated values until the values of $I_{o_i}\bar{\tau}_i(x_j)$ match the observed values $\left(B_i/B_{b_i}\right)$ to within one of two convergence criteria on the sum of squares of the residuals and significant digits accuracy (ref. 9) of the independent variables.

Details of the analysis technique are given in the appendix.

5.2 Data Products

The final results of the data analysis program are a tabulated listing of data for each line involved in the comparison process and plots of the fitted lines showing both calculated and experimentally determined data. The tabulated data can also be displayed as functions of time to portray a history of the data and permit rapid identification of the onset of trends in the data. The tabulated data include the following: a listing of line positions for each line involved in the calculations, the optical mass or pressure calculated for each line, the instrument function model used (either resolution or effective apodization as defined in the appendix) and its modeled values, a note which identifies the particular values excluded from the calculation of the means, the calculated means, the standard deviations for the optical mass, pressure, and instrument function coefficients, and the resultant mixing ratio, χ.

Sample outputs from the retrieval procedure are given in table 2 and in figure 5. Detailed results and analyses are presented in section 6.

Sample output from the nonlinear least-squares program is shown in table 2. The results achieved by analyzing a single set of interferometer data from cell S/N 20 which contains NO with the resolution model and the effective apodization model are shown in tables 2(a) and 2(b), respectively. Table 2 shows that seven weak lines were used to get a mean optical mass with the standard deviation calculated as an estimate on the uncertainty in the results. The resolution obtained for the fit of each line is tabulated as well as the resolution mean and standard deviation. The results for the pressure lines are given showing that five lines were used in calculating the means and that one line was ignored in the final calculation of pressure because its value was too far from the mean. As in the optical mass analysis the resolution for each line is given, as well as the resolution mean and standard deviation. Finally, the mixing ratio is presented along with its associated standard error. Table 2 also provides a comparison of results obtained with the two instru-

ment function models when they are applied to a common set of interferometer data. It can be seen that the retrieved values of U, p_t, and χ agree between the two models to within 5.5 percent for each parameter.

Sample data plots are given in figure 5. A sample line fit plot is shown in figure 5(a) where a typical fit of a line in the NO spectrum is indicated. Figure 5(b) is an identification diagram to assist in interpreting the parameters shown in figure 5(a). The column headed SIM displays the parameter values used by the program when it generates its own data. (Simulated line data are not generally used, but this mode was utilized for the contaminant study discussed in section 6.) The GUESS column gives the values used as inputs for the nonlinear least-squares program. A value of -999 in the GUESS column indicates that the parameter is not allowed to relax but is held constant at the value given in the SIM column; for example, the pressure is held fixed at 0.1 atm because this spectral line is used in the determination of the optical mass. The third column, FIT, is a listing of the results from the nonlinear least-squares program. The history of the optical mass, pressure, and mixing ratio for HCl cell S/N 21 is given in figure 5(c). The standard deviation of the data is denoted by an error bar. The cell nominal fill conditions are indicated by a long-dashed line which is used as a reference. The scale at the right end of the graph is used to show the percent difference from the nominal fill conditions. The short-dashed line gives the mean value based on the historical data. The data used to generate figure 5(c) were obtained with the resolution model and the fluctuations of the data about the mean are typical of the fluctuations inherent in the use of this model.

6 RESULTS

The HALOE gas cell life test program began in October 1980 and will continue until 1987. The program has, however, already yielded several significant results which warrant presentation at this time.

For convenience the results pertinent to each fill gas, namely, NO, CH_4, HCl, and HF, are presented in the following sections. In addition to the data from the life test program already described, each section shows the results of a contamination study which was performed with the life test gas cells. During this study, spectral data were obtained for each cell. These data covered most of, if not all, the spectral range of interest to the HALOE correlation channels (1800 to 4200 cm^{-1}). With these data, it was possible to determine the presence of contaminant gases (which absorb in the spectral range of interest) in the cells and in many cases to quantify their concentrations.

The results given below meet the accuracy requirements specified in section 5. It should be noted, however, that the accuracy of the results depends on the number of spectral lines being analyzed, since statistically the more spectral lines which are fit, the better the results will be. Because of the gas concentrations and individual characteristics of the absorption bands involved, the number of spectral lines available for analysis varies significantly; for the cells filled with 10 percent NO, approximately 6 spectral lines are available for optical mass calculations, but for the cells filled with 50 percent HF, only 2 lines (one each in the P and R branches) are available for optical mass calculations. Because of this, the calculations of the NO optical mass are considered to be somewhat more accurate than the corresponding HF calculations.

The accuracy of the results is also dependent on the spectral region in which the data are taken because of interferometer detector sensitivity and aperture effects. In general, the NO data are the least noisy and the least influenced by nonoptimum performance of the interferometer while the HF data are the most noisy and the most influenced by interferometer performance; the CH_4 and HCl data are moderately influenced by these effects.

Finally, the retrieved data given in the following subsections were obtained with the resolution model (see appendix) for the instrument function. Thus, the data presented have more scatter than they would have if the effective apodization model had been available when the data were being reduced. The early data can be reanalyzed with the effective apodization model if it becomes important to do so; to date, the difference in the scatter has not impacted the test program results.

6.1 NO Results

Four NO gas cells are used in the life test program, all filled to the same nominal conditions (table 1). The calculated mean optical mass, pressure, and mixing ratio plus the standard deviation for each, for all NO cell analyses performed prior to December 31, 1981, are given in table 3. A typical NO spectral plot from the interferometer is shown in figure 6.

The results in table 3 show that the derived optical mass of all cells is lower than the nominal fill condition by approximately 10 percent (consequently the derived pressures are approximately 10 percent high) and the accelerated aging test on cell S/N 21 did not produce any measurable change in the cell pressure and optical mass. The discrepancies between the nominal fill conditions and the retrieved values are believed to be caused by a combination of factors: measurement inaccuracies during the filling of the cells, inaccuracies in the line parameters used in the retrieval procedure, deficiencies in the instrument function model, and aliasing of the data from the interferometer. The contribution from each of these sources will require further study and definition.

The historical records for the NO cells are shown in figure 7. It can be seen that within the scatter of the data, there is no loss of NO from any of these cells.

A typical spectral survey for NO is shown in figure 8. The two features at wave numbers between 2200 and 2400 cm^{-1} have been identified as N_2O and CO_2 and the feature at approximately 3700 cm^{-1} is the 2-0 band of NO. The N_2O and CO_2 features are present in all NO cells but since the NO concentration is stable there is no apparent conversion to N_2O and no degradation of the NO concentration stability in the cell. The gradual decrease in the background level for wave numbers below 2200 cm^{-1} is caused by the optical filters in the interferometer. At the higher wave numbers, the background is dominated by electronic noise. An analysis of the spectrum shown in figure 8 gives a value of 400 ppm for the concentration of N_2O and 100 ppm for the concentration of CO_2.

6.2 CH_4 Results

Nine CH_4 gas cells are used in the life test program: four of these are filled with CH_4 at a mixing ratio of 1.0 and a pressure of 0.8 atm, the other five cells are filled with CH_4 at a mixing ratio of 0.5 and a pressure of 0.2 atm (table 1). The calculated mean optical mass, pressure, and mixing ratio plus the standard deviation

for each, for all the CH_4 cell analyses performed prior to December 31, 1981, are given in table 4. A typical CH_4 spectral plot is presented as figure 9.

As table 4 shows, the results of the analysis are available for only three of the four cells which contain undiluted CH_4. The fourth cell was not available to the life test program prior to preparation of this report.

Table 4 does not contain any data from the cells containing only 50 percent CH_4 because it has not been possible to obtain unique values for the specific set of spectral lines needed for analysis of the CH_4:N_2 cells. This has highlighted a potential problem for the HALOE data analysis since the conditions in these cells must be known before the HALOE atmospheric HCl data can be analyzed. These five cells are monitored at regular intervals; the data are stored on tape for future analysis and the spectral data are graphed. Visual examination of these plots has shown that there is no indication of a significant change in the cell pressure or CH_4 concentration.

From table 4, it can be seen that the derived values of the pressure, optical mass, and mixing ratio for the three cells analyzed agree with the nominal values. Thus, there is no indication of cell leakage or chemical reactions despite the fact that cell number 12 completed the thermal cycling test during this time.

The historical records for the three cells in table 4 are given in figure 10. It can be seen that within the scatter of the data, there is no loss of CH_4 from any of these cells.

A typical spectral survey for CH_4 is shown in figure 11. No contaminants are present in quantities sufficient to be observed above the background noise and the strong CH_4 spectral features. The implication is that if water vapor or other contaminants are present in these cells, they are present at concentrations of less than a few hundred ppm, based on an analysis of the data which included the noise level of the interferometer.

6.3 HCl Results

Five gas cells which contain HCl are used (table 1). The results of the analysis of the data from these cells are shown in table 5, and a typical HCl spectrum is shown in figure 12. Unlike the analyses of NO and CH_4, the P and R branches are analyzed separately except for cell S/N 21, which has only a few lines that can be used in the analysis because of the low optical depth and mixing ratio in this cell. The results in table 5 show that the pressure values retrieved from the R branch analyses are apparently lower than the pressure retrieved from the P branch analyses; the optical mass in cell S/N 19 appears to be 5 to 10 percent higher than the optical mass in cells 10 and 18, which are nominally filled to the same conditions; and none of the cells has exhibited any measurable change in pressure or optical mass over the lifetime of the cell. The apparent discrepancy in the pressures retrieved from the R branch data and the P branch data has been attributed to the previously mentioned inadequacies in the available line parameter data. The fact that there is no apparent change in the pressure or optical mass is significant since cell S/N 18 has completed both the accelerated aging and thermal cycling tests with no evidence of change. This is a strong indication that the gold cells will be suitable for the long-term containment of HCl.

The historical records for HCl cells S/N 10, 18, 19, 20, and 21 are given in figures 13 and 5. It can be seen that within the scatter of the data, there is no loss of HCl from these cells.

The survey spectra for the five cells were checked for indications of contaminants in the cells. One cell (S/N 18) showed the presence of water vapor in a concentration large enough to be detected above the spectral noise (fig. 14). The survey spectrum from a second cell (S/N 20) showed the possible presence of water vapor at the spectral noise level. The possibility that this water vapor was inside the interferometer and outside the gas cell was explored by both analysis and experiment. The instrument purge rate with dry nitrogen was increased and a cold trap was installed to reduce the water vapor concentration as much as possible. Good agreement between the water vapor line shapes generated by the program and the data was achieved by using combined HCl and N_2 broadened half-widths for water vapor. Since half-widths for H_2O broadened by HCl were unavailable in the literature, these half-widths were calculated with the aid of the nonlinear least-squares program. As a result of this investigation it was determined that cell S/N 18 contains approximately 2000 ppm of water vapor and cell S/N 20 contains at most a few hundred ppm. No other contamination has been observed in any of the HCl cells. The source of this contamination must be attributed to residual water vapor from the cell fabrication and cleaning processes since cells S/N 18 and 10 were filled on the same day and from the same source of HCl. Thus, cell fabrication and cleaning are also the probable sources of contamination for cell S/N 20. When filling the flight cells it will be important to provide adequate bake out under vacuum to insure that the cells are dry prior to filling.

6.4 HF Results

Five cells (table 1) which contain HF are used. The determination of the HF concentration in these cells was made by using spectral data at approximately 4000 cm^{-1}. No optimum optical filter was available for this spectral region and it was found to be necessary to measure the P branch and the R branch separately with two different optical filters. These considerations meant that the results of the analyses of the data for the two branches were potentially different because of instrument performance and corresponding slight differences in the values derived by the instrument line shape function model. Furthermore, the uncertainties in the line parameter values available for HF are greater than the uncertainties in the line parameter values for the other gases. Because of these uncertainties, the HF data were analyzed by using a "best fit" set of line parameters generated by adjusting the available data to allow agreement between theoretical and experimental line shapes. The problems and uncertainties just mentioned indicate that the uncertainties in the HF results are larger than the uncertainties in the results for NO, CH_4, and HCl. Figure 15(a) which shows the P branch and figure 15(b) which shows both the P and R branches of the HF spectrum for cell S/N 15 are typical of the HF spectra obtained for cells S/N 15, 16, and 17.

The results of the analyses are given in table 6. It can be seen that within the uncertainty of the analysis, the three cells filled to 0.2 atm pressure and 1.0 atm-cm optical mass are filled to the same conditions. The fact that the retrieved optical mass and mixing ratio are approximately 10 percent lower than the nominal fill conditions can be attributed to a combination of initial fill measurement errors, line parameter uncertainties, and the use of the resolution model for the instrument function model. There is no indication of a loss of HF in cells

S/N 15, 16, or 17 despite the fact that cell S/N 16 was exposed to an extended accelerated aging test.

Table 6 also shows that cells S/N 22 and 23 have lost a substantial amount of HF from their initial fill. The mixing ratio of cell S/N 22 is down by a factor of 20 from its nominal fill conditions and cell S/N 23 is down by a factor of 5. The loss of HF in these cells has been monitored by determining the optical mass as a function of time as shown in figure 16. It can be seen that the rate of the decrease was very fast immediately after the cell was filled but became very slow as time progressed. The available data for S/N 23 (table 6), and the fact that the spectral lines used for determining the optical mass in S/N 22 have not broadened with time, are taken as indicators of the integrity of the cells. It is believed that the reduction in HF is being caused by wall sorption effects and by reactions with the chrome and foreign materials left from the fabrication and cleaning processes. Cells S/N 15, 16, and 17 were examined for similar losses but none were detected. The amount of HF lost in cells S/N 22 and 23 was found to be less than the detection capability of the analyses procedures when applied to the higher concentrations in cells S/N 15, 16, and 17; that is, the total optical mass change in S/N 22 and 23 is less than 0.4 percent of the optical mass in S/N 15, 16, and 17. Based on these data it seems likely that cells S/N 15, 16, and 17 have lost small amounts of HF to the walls and to chemical reactions. Future data will be analyzed carefully to monitor for losses attributable to this cause. The historical records for HF cells S/N 15, 16, and 17 are given in figure 17. It can be seen that within the scatter of the data, the cells appear to have their original fill pressure and mixing ratio.

6.4.1 HF cell contamination study.- The survey spectra (figs. 18, 19, and 20) show that cells S/N 15, 16, and 17 contain measurable levels of contaminants which were identified as CO_2, HCl, HCN, CH_4, and H_2O. The retrieved concentrations of these contaminants obtained by using the nonlinear least-squares method are given in table 7. The determination of the water vapor content was particularly difficult since the half-width data for H_2O broadened by HF were not available and since water vapor inside the interferometer can affect the experimental data. In order to estimate the water vapor in the cells, experimental data were obtained while using the cold trap to reduce the water vapor in the interferometer to a minimum and then retrievals were performed to determine the effective (HF and N_2 broadened) half-widths of water vapor lines in these spectra. The concentrations of the other contaminants (CO_2, HCl, CH_4, and HCN) shown in table 7 were derived by assuming the effective half-widths to be the same as the N_2 broadened half-widths, since data on HF-broadened half-widths for these species were unavailable.

As part of the overall contamination study, cell S/N 16 was heated slightly while inside the interferometer and the water vapor observed with the cell in the heated condition and again after the cell was cooled to ambient temperature. The water vapor increased to approximately 5000 ppm when the cell was heated and then decreased again as the cell cooled. This is believed to be due to the outgassing and reabsorption of water vapor trapped on the interior cell walls during the fabrication and cleaning processes.

The source of the contaminants (table 7) was studied. It was found that the CO_2, HCl, CH_4, and some H_2O were impurities in the bottle of HF gas used to fill the cells. The HCN is apparently the result of having cyanide from the plating solution trapped in the gold cell walls during the fabrication process. It is theorized that the HF migrates into the gold surface and leaches the HCN out of the gold. The HCN concentration has not changed since it was first observed and it appears that the HCN

leach-out process is self-limiting and can probably be overcome by adequate passivation prior to the filling of flight cells.

Three other features appear in the HF cell spectral data taken at room temperature. The first (fig. 15(a)) at wave numbers from 3600 to 3690 cm^{-1} has been tentatively identified as a $HF \cdot H_2O$ complex (ref. 11). The second (fig. 15(b)) at wave numbers from 3800 to 3950 cm^{-1} has been tentatively identified as the HF dimer (ref. 12). The spectrum from cell S/N 16 in the wave-number region between 2650 and 3100 cm^{-1}, presented in figure 21, shows the presence of HCl in this cell. The cause of the broad feature between wave numbers 2900 and 3000 cm^{-1} (also seen in figs. 19 and 20) has been tentatively indentified as a complex composed of HF and CH_4 molecules. The formation of these complexes represents a potential HF loss mechanism and reinforces the importance of removing contaminants from the fill gases.

6.4.2 Thermal effects test results.- Cell S/N 15 was exposed to a reduced temperature thermal effects test. The spectrum from this test (fig. 22) shows features which were not seen in figures 15(a), 15(b), or 21. These have been identified as HF tetramer and HF hexamer (ref. 12). At 270 K, the HF monomer concentration has been reduced by approximately 5 percent as conversion to the polymer form takes place. In figure 23, the percent change in optical mass is compared with that predicted by the gas law. Since the optical mass is proportional to pressure and, from the perfect gas law, the pressure is proportional to temperature for a given volume, it follows that a change in optical mass is proportional to a change in temperature if HF behaves as a perfect gas. Because of conversion to a polymer form, HF is not a perfect gas and, as figure 23 shows, the optical mass deviates from the percent change predicted by the perfect gas law. At 260 K, the conversion causes a monomer loss of approximately 20 percent. This factor is important for the analysis of the flight data from HALOE and dictates that the temperature of the gas cells must be monitored.

Two of the spectral features noted in figures 15(a) and 15(b) were studied as the cell temperature was lowered. The feature at approximately 3850 cm^{-1} became more pronounced; this indicated that the amount of HF dimer in the cell increased as expected. The feature at approximately 3600 cm^{-1}, on the other hand, became less prominent at lower temperatures and was not discernible above the spectral noise at temperatures below approximately 280 K. This behavior is similar to the behavior of water vapor in the cell. Thus, it was inferred that the feature at 3600 cm^{-1} was indicative of the presence of water vapor in the cell, as would be expected if a $HF\ H_2O$ complex was present. The decrease in concentration at the lower temperatures is probably caused by "freezing out" of the water molecules on the wall. At the present time, it is not known whether this complex will have a significant effect on the HALOE data analysis. The HF CH_4 complex was not recognized at the time the thermal effects tests were being conducted so that there are presently no data on the behavior of this complex with temperature.

Cell S/N 22 was also subjected to temperatures down to 260 K while in the interferometer. The data show a reduction of HF optical mass both as a function of temperature and as a function of the amount of time at the reduced temperature (fig. 24). The percentage reduction in the HF optical mass in cell S/N 22 is approximately the same as the percentage reduction in HF in cell S/N 15 for the same time (approximately 1/2 hour) at the lowest temperature (fig. 23). Extending the time (up to 70 hours) at the reduced temperature on cell S/N 22 showed a further reduction in the HF concentration in the cell. Further tests and analyses will be required to establish that this effect is real and not caused by scatter in the data. Furthermore, if the effect is shown to be real, it will be desirable to determine the cause

of the HF reduction. At the present time, it is not possible to distinguish between HF concentration reduction due to polymer formation and HF concentration reduction due to increased wall sorption effects at the reduced temperature. It is important to note that for both HF cells S/N 15 and 22, the HF concentration returned to its original value (within measurement accuracy limits) when the cell temperature was returned to room conditions.

These thermal effects tests have yielded extremely valuable data for the HALOE instrument and the HALOE HF channel data analysis. The test results have shown that the gas cell temperatures in the HALOE instrument must be controlled to avoid thermal effects which can introduce nonlinear perturbations in the optical mass of the gas cell. The results have also shown that the cell temperatures must be monitored during a data event and that these temperatures will influence the retrieved optical mass. At the present time, these results are based only on the results from two HF gas cells. Further research is required to quantify the extent of these effects and provide detailed information to the instrument design and data analysis activities. It is also important that a similar set of tests be conducted for the other gases.

6.4.3 Gold laminate deterioration.- After cell S/N 16 completed the accelerated aging test (400 hours at 85°C) it was observed that the gold layer overcoating the chrome substrate on the sapphire windows (fig. 3) was "blistering"; this indicates that the gold was being delaminated from the chrome in local areas. The heat was reapplied for an additional 300 hours at which time the deterioration seemed to have stabilized and the test was discontinued. This same deterioration has since been observed to some extent in all cells which contain HF and is attributed to chemical reactions between the HF and the chrome in the layer between the gold and the sapphire. Furthermore, it has been observed that the deterioration has not stabilized in cell S/N 16 but is progressing at a very slow rate. Because of this, the continuing growth of the blistering is monitored constantly. The extended heating of cell S/N 16 has given this cell a "chemical age" of over 5 years with no apparent loss of HF so that there is no reason to believe that this represents a serious failure mechanism for the flight cells.

7 CONCLUDING REMARKS

The Halogen Occultation Experiment (HALOE) will use gas-filter correlation radiometry to measure the atmospheric concentration profiles of HCl, HF, NO, and CH_4 from the Upper Atmosphere Research Satellite. Because the containment of these gases in gas-filter cells for an extended period of time (several years) has never been attempted before, a gas cell life test program is underway at Langley Research Center as part of the HALOE program. The primary objectives of this test program are to demonstrate the integrity of the cells and the stability of the gases in the cells by exposing filled cells to simulated storage and flight environments and to identify any contaminants which might be present in the filled cells so that their impact can be assessed and their sources found and eliminated.

The gas cell life test program began in October 1980 and the gas cells in the program have been monitored at regular intervals and at specific times, depending on the individual test being conducted. The test program consists of a set of five tests which, in combination, permit the program objectives to be met.

The primary data from all tests in the program are the infrared spectra of the gases in the cells. These spectra are produced by a Fourier Transform Infrared Interferometer. The data from the interferometer must be analyzed in terms of the

concentration of the gases in the cells. An extensive analysis procedure was developed to analyze the interferometer data and produce values of the optical mass, pressure, and mixing ratio of the gases in each cell. This report provides a description of the methodology developed for the analysis program and a summary of the test program results through December 1981.

The test program results to date can be summarized as follows:

1. There were no indications of leaks in any cell through the end of 1981.

2. There are no significant anomalies in the CH_4 and NO cells. All these cells appear to be filled to the specified conditions and are maintaining those conditions.

3. The only anomaly observed for the HCl cells is the presence of approximately 2000 ppm of water vapor in one cell and possibly trace amounts of water vapor in another cell. The source of this contamination is believed to be residual water vapor from the fabrication and cleaning processes.

4. Three of the HF cells are filled to nominal conditions of 0.2 atm and 0.5 mixing ratio. There is no measurable change in the amount of HF in these cells despite the fact that one of these cells has been heated to 85°C for 700 hours. These cells contain small but measurable amounts of contaminants: HCl, HCN, CH_4, CO_2, and H_2O, which do not affect the data reduction process for the life program but may be very significant to the HALOE data reduction. The source of these contaminants was found to be partially caused by contamination in the HF source gas and partially caused by the action of HF in leaching out residual plating bath materials trapped in the gold walls. Elimination or significant reduction in the levels of HCl, CH_4, CO_2, and H_2O in the flight gas cells will require an ultrapure source and meticulous attention to detail during the filling process. It is believed that the HCN concentration will be eliminated or significantly reduced by the passivation process needed to eliminate wall sorption effects.

5. Two of the HF cells are filled to very low pressure and optical mass, and these cells have shown a reduction in HF concentration but with no increase in cell total pressure. Based on this, it is believed that the HF is being absorbed by the cell walls or is reacting with other materials in the cells, viz, a chrome underlayer used in the cell construction to help the gold adhere to the sapphire windows, or the residue from other materials used in the cell fabrication process. Losses due to HF adsorption or absorption by the cell walls may be eliminated by adequate passivation prior to filling the cell. Losses due to chemical reactions cannot be entirely prevented but can be minimized by proper construction and cleaning prior to fill.

6. Two of the HF cells have been exposed to temperatures from 300 K to 260 K. At reduced temperatures, the measured optical mass deviates from that predicted by the perfect gas law because of the formation of HF polymers with a consequent reduction in the HF monomer concentration. This indicates a need for thermal control of the gas cells in the HALOE instrument, and a need for gas cell temperature data as part of the HALOE data-reduction process.

7. All the HF cells show a deterioration in the form of blisters in the gold ring which is deposited over a chrome sublayer around the periphery of the sapphire windows. This deterioration is attributed to chemical reactions between the HF and the chrome. The deterioration is continuing but, since one cell was heated to 85°C for 700 hours with no change of total pressure or optical mass, this is not considered a serious threat to the cell life expectancy.

8. The analysis of the data from the interferometer led to the conclusion that better spectral parameters (line position, line strength, and half-width) are needed for all the gases in the cells. In particular, it was found that the data from the CH_4 cells filled to a mixing ratio of 0.5 (diluent is N_2) cannot be analyzed because the required spectral data (i.e., nitrogen broadened half-widths) are not currently available. This may be an important consideration for the HALOE data-reduction process.

The life test program will continue until 1987. The tests involving thermal cycling and accelerated aging will be completed as quickly as possible. After these tests are complete, the cells will be kept in ambient temperature storage until the end of the program.

Langley Research Center
National Aeronautics and Space Administration
Hampton, VA 23665
May 20, 1983

APPENDIX

METHOD OF ANALYZING INTERFEROMETER DATA

A.1 Outline of Procedure

As stated in section 5, the interferometer data are analyzed with a nonlinear least-squares technique which minimizes the differences $f(x_j)$ between observed and theoretical spectra. The differences are given by

$$f(x_j) = \frac{B_i}{B_{b_i}} - I_{o_i} \bar{\tau}_i(x_j) \tag{A1}$$

where

i = 1, 2, ..., N sample data points

x_j independent parameters

j = 1, 2, ..., M

B_i observed radiance incident on interferometer detector with gas cell in place (single beam spectrum)

B_{b_i} observed radiance incident on interferometer detector with empty gas cell in place (single beam spectrum)

$\frac{B_i}{B_{b_i}}$ ratio of radiances, raw data from interferometer

I_{o_i} fitted background of spectrum to account for small differences in cell window transmission between filled and empty cells and for interferometer signal amplitude stability between interferograms

$\bar{\tau}_i(x_j)$ calculated transmittance convolved with instrument line-shape function; a function of line position, strength and half-width, pressure, path length, gas mixing ratio, and instrument line shape

The technique developed for analysis of the data involves modeling $\bar{\tau}_i(x_j)$ and I_{o_i} such that their product equals $\frac{B_i}{B_{b_i}}$.

APPENDIX

A.2 Calculation of Transmittance

The calculated transmittance is given by the following equation:

$$\bar{\tau}_i(x_j) = \int_{-\infty}^{\infty} \tau(\nu')\, \Phi(\nu_i - \nu')\, d\nu' \tag{A2}$$

where

$\tau(\nu')$ infinite resolution transmittance

$\Phi(\nu_i - \nu')$ instrument line shape function

ν wave number, cm^{-1}

the transmittance $\tau(\nu')$ is defined as

$$\tau(\nu') = \exp[-K_{\nu'}(\nu_o, p_t)U] \tag{A3}$$

where

$K_{\nu'}$ absorption coefficient, function of line strength, line position, and half-width

ν_o line position

p_t cell total pressure, $p_s + p_N$

U optical mass, $p_t \chi \ell$

χ volume mixing ratio of absorbing gas

p_s partial pressure of gas of interest

p_N partial pressure of nitrogen (diluent gas)

ℓ path length, length of cell

The absorption coefficient is calculated by using the Voight line shape (ref. 13). For the pressures involved in most of the cells in the life test program ($p_t \geq 0.1$ atm), the Voight line shape becomes the Lorentzian shape given by

$$K_{\nu'} = \frac{S\alpha/\pi}{\alpha^2 + (\nu - \nu_o)^2} \tag{A4}$$

where

$$\alpha = \frac{\alpha_s p_s + \alpha_N p_N}{p_s + p_N} \tag{A5}$$

S line strength

α_s self-broadened half-width

α_N nitrogen-broadened half-width

Values for S and ν_o are given in reference 14 for standard conditions of pressure and temperature p_o and T_o, and α_s and α_N are taken from the available literature as required. These values must be adjusted for the cell conditions p_t and T. This adjustment is made by using

$$\alpha_s(p_t,T) = \alpha_s(p_o,T_o)\left(\frac{p_t}{p_o}\right)\left(\frac{T_o}{T}\right)^{1/2} \tag{A6}$$

$$\alpha_N(p_t,T) = \alpha_N(p_o,T_o)\left(\frac{p_t}{p_o}\right)\left(\frac{T_o}{T}\right)^{1/2} \tag{A7}$$

Similarly S is adjusted for the cell conditions as follows:

$$S(T) = S(T_o)\left\{\left(\frac{T_o}{T}\right)^{\gamma} \exp\left[-1.439\left(\frac{T_o}{T} - 1\right)\frac{E}{T_o}\right]\right\} \tag{A8}$$

where

γ a constant depending on gas

E energy level given in reference 14

and the vibration partition function is not included because it is negligible for the temperature at which the spectra were taken. Equations (A4), (A5), (A6), (A7), and (A8) combined with the temperature and pressure are used to calculate K_ν, and then τ_ν, from equation (A3).

APPENDIX

A.3 Instrument Line-Shape Function

The instrument line-shape function $\Phi(\nu_i-\nu')$ comes from three effects resulting from the use of the interferometer (ref. 8): (1) truncation of the interferogram caused by the maximum path length difference (mirror travel) L, (2) the instrument apodization function used to reduce side lobes in the Fourier transformed spectrum which produces B_i and B_{b_i}, and (3) errors in the sampled interferogram due to optics misalignment, electronic noise, source fluctuations, and field-of-view averaging effects on the signal. In general,

$$\Phi(\nu_i-\nu') = 2\int_0^L A(\delta)\ F(\delta)\ \exp[-i2\pi\delta(\nu_i - \nu')]\ d\delta \tag{A9}$$

where

L maximum path length difference in interferometer

$A(\delta)$ known apodization function

$F(\delta)$ instrument function to account for errors noted

$\exp[-i2\pi\delta(\nu_i - \nu')]$ Fourier and inverse Fourier transform function

δ instantaneous path length

In equation (A9), the apodization function $A(\delta)$ is given by the Happ-Genzel function used by the interferometer manufacturer:

$$A(\delta) = 0.54 + 0.46 \cos\frac{\delta\pi}{L}$$

A.4 Instrument Function Model

It is a common experience that the spectral output from the interferometer is not precisely the same from one set of data to another. This is true even though neither the sample being analyzed nor the interferometer operating conditions are changed. Thus, there is a need for an instrument function model to account for the changes. Two such models have been developed for the analysis of the gas cell data.

Resolution Model: This model is based on the fact that the resolution of the interferometer is proportional to $1/L$. Thus, it was found convenient to set $F(\delta) = 1.0$ in equation (A9) and to permit the maximum difference in path length to vary while solving equations (A2) and (A1). This technique produces values of U, p_t, and χ which have scatter in excess of ±15 percent; it also results in values of L significantly different from the known maximum difference in path length (16 cm) and, hence, instrument resolution values significantly different from the theoretical value (0.060 cm^{-1}).

APPENDIX

Effective Apodization Model: The deficiencies noted in the resolution model, viz large scatter in the data and physically unrealistic values of L, highlighted a need for a better model for $F(\delta)$. After studying the data for over a year and trying many forms for $F(\delta)$, $F(\delta)$ was observed to be a randomly varying function of the sampled interferogram data points. It was also observed that any given set of data points had a trend which could be modeled by a straight line. Based on this observation, it was assumed that

$$F(\delta) = 1 + \frac{\delta}{L} D \tag{A10}$$

where D is allowed to vary during the solution of equations (A2) and (A1) and thus account for the variability of the trends in the data points. The application of equation (A10) had the effects of (1) reducing the scatter in the results to ±5 percent and (2) permitting L to remain fixed at the known value of 16 cm.

A.5 Fitted Background

Equation (A1) shows that the calculated transmittance must be adjusted for effects which change the background value of the spectrum: optical filter effects, Fabry-Perot effects from the gas cell windows, and variations in the interferometer source intensity. The background has been modeled with a linear function

$$I_o = B + C(\nu_o - \nu) \tag{A11}$$

where B and C are constants determined during the solution of equation (A1). When Fabry-Perot effects are significant a second background model is used:

$$I_o = \frac{I_{max}}{1 + \left(\frac{I_{max}}{I_{min}} - 1\right)\left[\sin^2 \frac{\pi}{W}(\nu - \beta)\right]} \tag{A12}$$

where

I_{max} maximum intensity level of Fabry-Perot pattern

I_{min} minimum intensity level of Fabry-Perot pattern

W distance in wave numbers between successive values of I_{max}, $\nu_{I_{max_1}} - \nu_{I_{max_2}}$

β wave number at which I_{max_1} occurs

The values of I_{max}, I_{min}, W, and β are determined during the solution of equation (A1).

A.6 Calculation Procedure

The calculation procedure used to solve equation (A1) is performed by the MARQ routine on the computers at the Langley Research Center. This routine, which is based on the Levenberg-Marquardt algorithm (ref. 9) is used to minimize the values of equation (A1) in selected spectral regions and to deduce the associated values of pressure, mixing ratio, and optical mass. The MARQ routine solves for values of the parameters until the residual sum of squares meets specified criteria or until the parameters do not vary from iteration to iteration to within a specified criterion. When the calculations are complete the data are tabulated (e.g., table 2), plotted (e.g., fig. 5(a)), and stored so that historical studies can be made (e.g., fig. 5(c)).

REFERENCES

1. Russell, James M., III; Park, Jae H.; and Drayson, S. Roland: Global Monitoring of Stratospheric Halogen Compounds From a Satellite Using Gas Filter Spectroscopy in the Solar Occultation Mode. Appl. Opt., vol. 16, no. 3, Mar. 1977, pp. 607-612.

2. Man's Impact on the Global Environment. Report of the Study of Critical Environmental Problems (SCEP). MIT Press, c.1970.

3. Inadvertent Climate Modification: Report of the Study of Man's Impact on Climate (SMIC). MIT Press, c.1971.

4. Grobecker, A. J.; Coroniti, S. C.; and Cannon, R. H., Jr.: Report of Findings - The Effects of Stratospheric Pollution by Aircraft. TST-75-50, U.S. Dep. Transp., Dec. 1974. (Available from DTIC as AD A005 458.)

5. Halocarbons: Effects on Stratospheric Ozone. Natl. Acad. Sci., 1976.

6. Stolarski, R. S.; and Cicerone, R. J.: Stratospheric Chlorine: A Possible Sink for Ozone. Canadian J. Chem., vol. 52, no. 8 (pt. 2), Apr. 15, 1974, pp. 1610-1615.

7. Molina, Mario J.; and Rowland, F. S.: Stratospheric Sink for Chlorofluoromethanes: Chlorine Atom Catalysed Destruction of Ozone. Nature, vol. 249, no. 5460, June 28, 1974, pp. 810-812.

8. Park, Jae H.: Analysis Method for Fourier Transform Spectroscopy. Appl. Optics, vol. 22, no. 6, Mar. 15, 1983, pp. 835-849.

9. Brown, K. M.; and Dennis, J. E.: Derivative Free Analogues of the Levenberg-Marquardt and Gauss Algorithms for Nonlinear Least Squares Approximation. Numer. Math., vol. 18, no. 4, 1972, pp. 289-297.

10. Chang, Y. S.; and Shaw, J. H.: A Nonlinear Least Squares Method of Determining Line Intensities and Half-Widths. Appl. Spectros., vol. 31, no. 3, May/June 1977, pp. 213-220.

11. Thomas, R. K.: Hydrogen Bonding in the Vapour Phase Between Water and Hydrogen Fluoride: The Infrared Spectrum of the 1:1 Complex. Proc. R. Soc. London, ser. A, vol. 344, no. 1639, Aug. 12, 1975, pp. 579-592.

12. Smith, D. F.: Hydrogen Fluoride Polymer Spectrum, Hexamer and Tetramer. J. Chem. Phys., vol. 28, no. 6, June 1958, pp. 1040-1056.

13. Drayson, S. R.: Rapid Computation of the Voigt Profile. J. Quant. Spectros. & Radiat. Transfer, vol. 16, no. 7, July 1976, pp. 611-614.

14. Rothman, L. S.: AFGL Atmospheric Absorption Line Parameters Compilation: 1980 Version. Appl. Opt., vol. 20, no. 5, Mar. 1, 1981, pp. 791-795.

SYMBOLS

ℓ	cell length, cm
p	cell pressure
p_t	cell total pressure, atm
U	optical mass, $p_t \chi \ell$, atm-cm
σ	standard deviation
χ	volume mixing ratio

Bar over symbol indicates mean value.

TABLE 1.- HALOE GAS CELL LIFE TEST PROGRAM PLAN

NO			CH_4			CH_4 (BLOCK)[a]			HCl			HF		
Cell S/N	p_t/χ (b)	Test (c)	Cell S/N	p_t/χ (b)	Test (c)	Cell S/N	p_t/χ (b)	Test (c)	Cell S/N	p_t/χ (b)	Test (c)	Cell S/N	p_t/χ (b)	Test (c)
20	0.1/0.1	A B C	11	0.8/1.0	E D	10	0.2/0.5	E D	10	0.1/0.1	E D	15	0.2/0.5	E D
21	0.1/0.1	A X B C	12	0.8/1.0	A D C X	13	0.2/0.5	A B	18	0.1/0.1	A X C X	16	0.2/0.5	A X D
22	0.1/0.1	B	25	0.8/1.0	B	14	0.2/0.5	A D C	19	0.1/0.1	A B D	17	0.2/0.5	A B C
23	0.1/0.1	E D	26	0.8/1.0	A B	18	0.2/0.5	A B C X	20	0.1/0.05	B	22	0.1/0.004	B
						27	0.2/0.5	B	21	0.05/0.01	A B C	23	0.05/0.008	A B C

[a]These cells are used to remove CH_4 interference from the HCl measurements.
[b]Nominal fill conditions: p_t = Total pressure in cell, atm; χ = Volume mixing ratio, diluent is N_2.
[c]Code: A - Heat to 85°C for 400 hours
B - Store under vacuum at room temperature
C - 2000 temperature cycles between 37°C and 7°C
D - Obtain spectra with cell at several temperatures between -15°C and 50°C
E - Store at room temperature and pressure
X - Test complete as of 12/31/81

TABLE 2.- SAMPLE TABULATED DATA

(a) Data retrieved with resolution model

Gas Cell S/N 20	Date of Scan: Aug. 31, 1981
Fill Gas: $NO:N_2$	Time of Scan: 8:50 AM
	Temperature of Scan: 28.7°C

Optical mass lines

Wave number, cm^{-1}	Optical mass, atm-cm	Resolution, cm^{-1}
1943.355	0.083874	0.066027
1945.897	.081969	.065320
1947.166	.082174	.065626
1948.399	.083160	.067061
1949.611	.080533	.065082
1950.863	.080767	.066098
1952.019	.079888	.064458
Mean, 0.081766 atm-cm; standard deviation, 0.01451 atm-cm Resolution mean, 0.065667 cm^{-1}; standard deviation, 0.000835 cm^{-1}		

Pressure lines

Wave number, cm^{-1}	Pressure, atm	Resolution, cm^{-1}
1924.451	0.108806	0.066268
1926.283	.110629	.066832
1927.270	.120128	[a].066204
1929.020	.111772	.066412
1934.385	.115204	.066397
Mean, 0.111603 atm; standard deviation, 0.002694 atm Resolution mean, 0.066477 cm^{-1}; standard deviation, 0.000245 cm^{-1} Mixing ratio, 0.07326546362791; standard deviation, 0.002195134128631		

[a]Not used in final average.

TABLE 2.- Concluded

(b) Data retrieved with effective apodization model

Gas Cell S/N 20	Date of Scan: Aug. 31, 1981
Fill Gas: $NO:N_2$	Time of Scan: 8:50 AM
	Temperature of Scan: 28.7°C

Optical mass lines

Wave number, cm^{-1}	Optical mass, atm-cm	Effective apodization
1943.355	0.087413	-0.270257
1945.896	.084945	-.251017
1947.166	.085314	-.244281
1948.399	.090090	[a]-.377778
1949.611	.082968	-.215983
1950.863	.085994	-.293187
1952.019	.083303	-.220517
Mean, 0.084989 atm-cm; standard deviation, 0.001669 atm-cm Effective apodization mean, -0.249207; standard deviation, 0.029434		

[a]Not used in final mean.

Pressure lines

Wave number, cm^{-1}	Pressure, atm	Effective apodization
1924.451	0.113526	-0.290959
1926.283	.115098	-.288376
1927.270	.124664	-.290149
1929.020	.115629	-.275715
1934.386	.121579	-.296683
Mean, 0.118099 atm; standard deviation, 0.004776 atm. Effective apodization mean, -0.288376; standard deviation, 0.007732 Mixing ratio, 0.07196437014492; standard deviation, 0.003235151308938		

TABLE 3.- RESULTS OF ANALYSES OF NO GAS CELL DATA FOR PERIOD ENDING DECEMBER 31, 1981

[Nominal fill conditions (all cells): U = 0.1 atm-cm; p_t = 0.1 atm; χ = 0.1]

Cell S/N	Spectral data sets used in determining mean values	$\bar{U} \pm \sigma$, atm-cm	$\bar{p} \pm \sigma$, atm	$\bar{\chi} \pm \sigma$
20	9 R branch	0.0880 ± 0.0043	0.106 ± 0.0053	0.0830 ± 0.0071
[a]21	13 R branch	.0872 ± .0038	.108 ± .0041	.0808 ± .0053
22	10 R branch	.0872 ± .0025	.107 ± .0036	.0815 ± .0039
23	10 R branch	.0872 ± .0030	.109 ± .0032	.0803 ± .0042

[a]Accelerated aging test cell.

TABLE 4.- RESULTS OF ANALYSES OF CH_4 GAS CELL DATA FOR PERIOD ENDING DECEMBER 31, 1981

[Nominal fill conditions (all cells): U = 8.0 atm-cm; p_t = 0.8 atm; χ = 1.0]

Cell S/N	Spectral data sets used in determining mean values	$\bar{U} \pm \sigma$, atm-cm	$\bar{p} \pm \sigma$, atm	$\bar{\chi} \pm \sigma$
[a]12	10 P branch	7.98 ± 0.13	0.793 ± 0.0096	1.01 ± 0.026
25	7 P branch	8.01 ± .19	.794 ± .013	1.01 ± .040
26	7 P branch	7.97 ± .18	.799 ± .011	.998 ± .035

[a]2000 temperature cycle test cell.

TABLE 5.- RESULTS OF ANALYSES OF HCl GAS CELL DATA FOR PERIOD ENDING DECEMBER 31, 1981

Nominal fill conditions:
S/N 10, 18, and 19: $U = 0.1$ atm-cm; $p_t = 0.1$ atm; $\chi = 0.1$
S/N 20: $U = 0.05$ atm-cm; $p_t = 0.1$ atm; $\chi = 0.05$
S/N 21: $U = 0.005$ atm-cm; $p_t = 0.05$ atm; $\chi = 0.01$

Cell S/N	Spectral data sets used in determining mean values	$\bar{U} \pm \sigma$, atm-cm	$\bar{p} \pm \sigma$, atm	$\bar{\chi} \pm \sigma$
10	18 P branch	0.0967 ± 0.0067	0.106 ± 0.0058	0.0914 ± 0.0081
10	15 R branch	.0948 ± .0052	.0968 ± .0040	.0981 ± .0067
[a]18	15 P branch	.0973 ± .0064	.106 ± .0051	.0918 ± .0072
[a]18	13 R branch	.0961 ± .0051	.0948 ± .0033	.101 ± .0072
19	10 P branch	.103 ± .0053	.105 ± .0028	.0983 ± .0055
19	14 R branch	.102 ± .0064	.0958 ± .0047	.107 ± .011
20	15 P branch	.0529 ± .0040	.107 ± .0053	.0491 ± .0028
20	14 R branch	.0523 ± .0026	.0962 ± .0058	.0547 ± .0046
21	16 both P & R	.00482 ± .00033	.0486 ± .0026	.00983 ± .00088

[a]Accelerated aging and 2000 cycle temperature test cell.

TABLE 6.- RESULTS OF ANALYSES OF HF GAS CELL DATA FOR PERIOD ENDING DECEMBER 31, 1981

[Nominal fill conditions:
S/N 15, 16, 17: U = 1.0 atm-cm; p_t = 0.2 atm; χ = 0.5
S/N 22: U = 0.004 atm-cm; p_t = 0.1 atm; χ = 0.004
S/N 23: U = 0.004 atm-cm; p_t = 0.05 atm; χ = 0.008]

Cell S/N	Spectral data sets used in determining mean values	$\bar{U} \pm \sigma$, atm-cm	$\bar{p} \pm \sigma$, atm	$\bar{\chi} \pm \sigma$
15	18 P branch	0.889 ± 0.062	0.199 ± 0.022	0.452 ± 0.056
15	12 R branch	.854 ± .045	.178 ± .013	.482 ± .039
[a]16	28 P branch	.918 ± .076	.198 ± .027	.473 ± .083
[a]16	14 R branch	.880 ± .063	.191 ± .019	.462 ± .042
17	15 P branch	.898 ± .069	.195 ± .033	.475 ± .089
17	14 R branch	.863 ± .065	.199 ± .023	.439 ± .053
[b]22	Both P & R	.000207 ± .000011 (most recent)	.100 assumed	.000207 ± .000011 (most recent)
[b]23	Both P & R	.000770 ± .000030 (most recent)	.0513 ± .0035 (most recent)	.00150 ± .00012 (most recent)

[a]Accelerated aging test cell - extended test time.

[b]Values given are for a single (most recent) set of data; HF S/N 22 historical record is based on 16 data sets, HF S/N 23 historical record is based on 13 data sets.

TABLE 7.- CONCENTRATIONS OF CONTAMINANTS IN THE HF GAS CELLS

[Spectra for CO_2, HCl, CH_4, HCN taken on 8/19/81; spectra for H_2O taken on 3/18/81 and 5/27/81]

Cell S/N	Concentration, ppm, of -				
	CO_2	HCl	CH_4	HCN	H_2O (a)
15	50	200	[b]50	200	2000
16	400	1300	400	1000	3000
17	200	1300	400	1000	2000

[a]Water values are upper limits. Exact determination depends on quality of purge and half-widths values.

[b]Upper limit. No visible spectra above background noise.

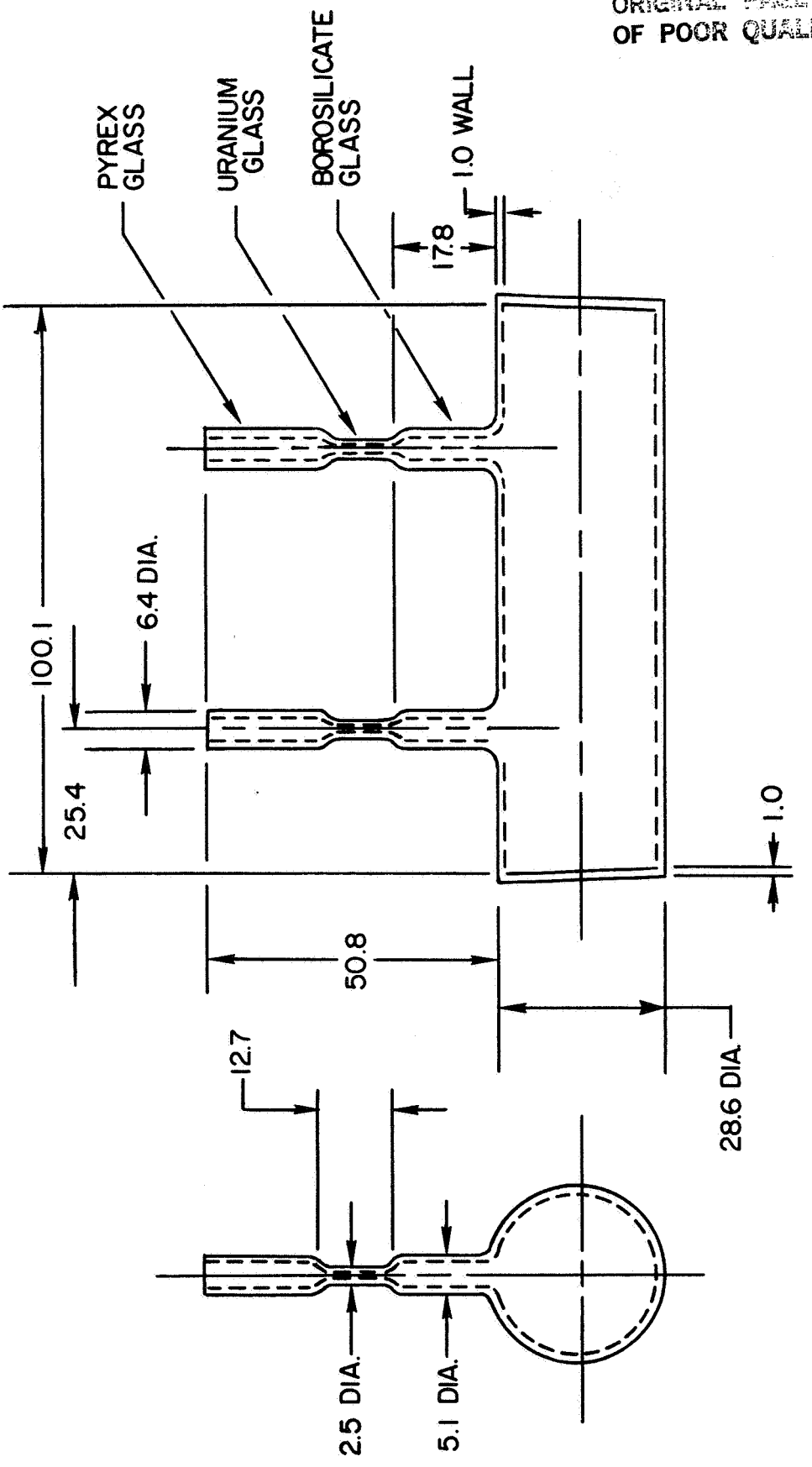

Figure 1.- Glass cell design. Dimensions are in millimeters.

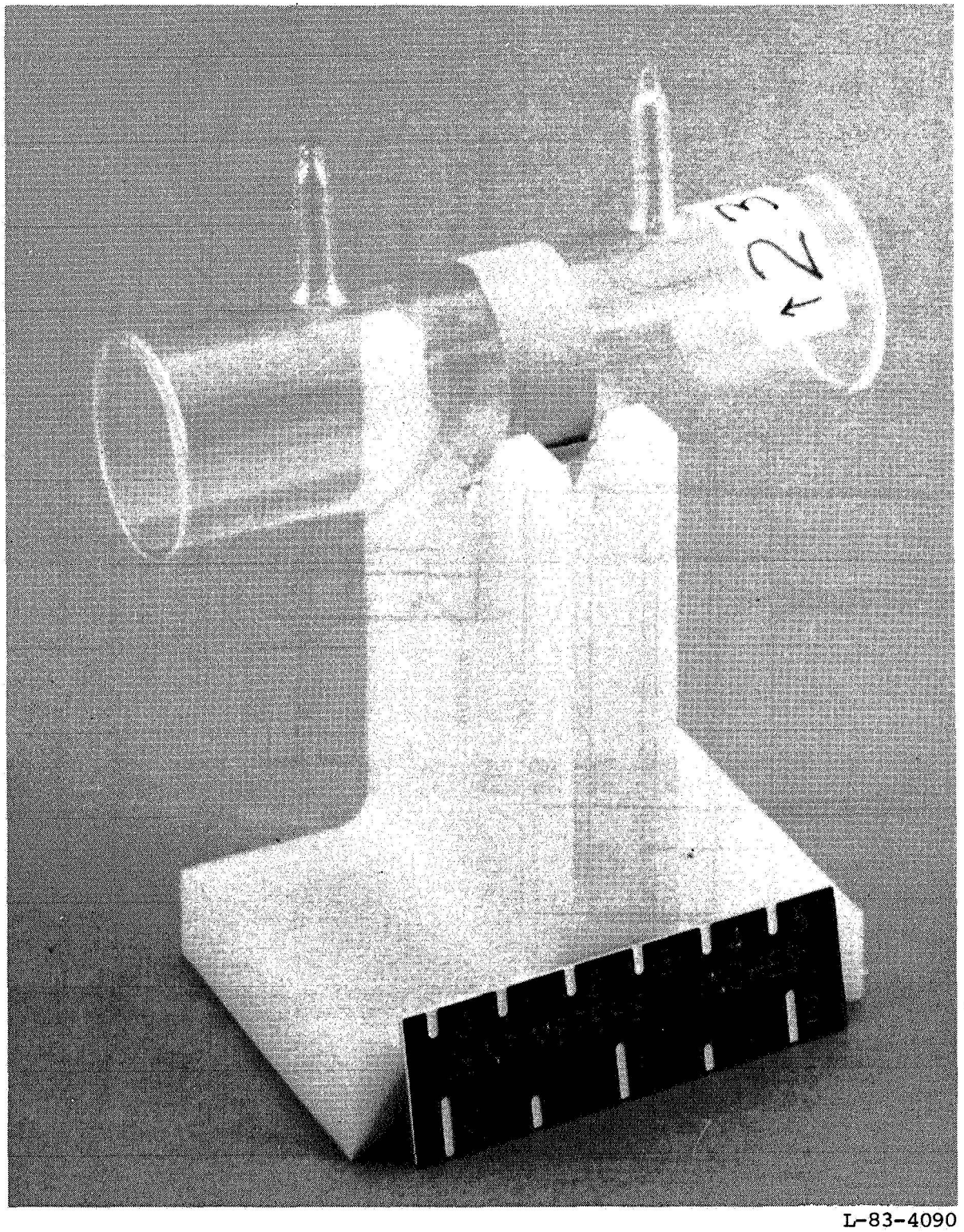

L-83-4090

Figure 2.- Glass cell.

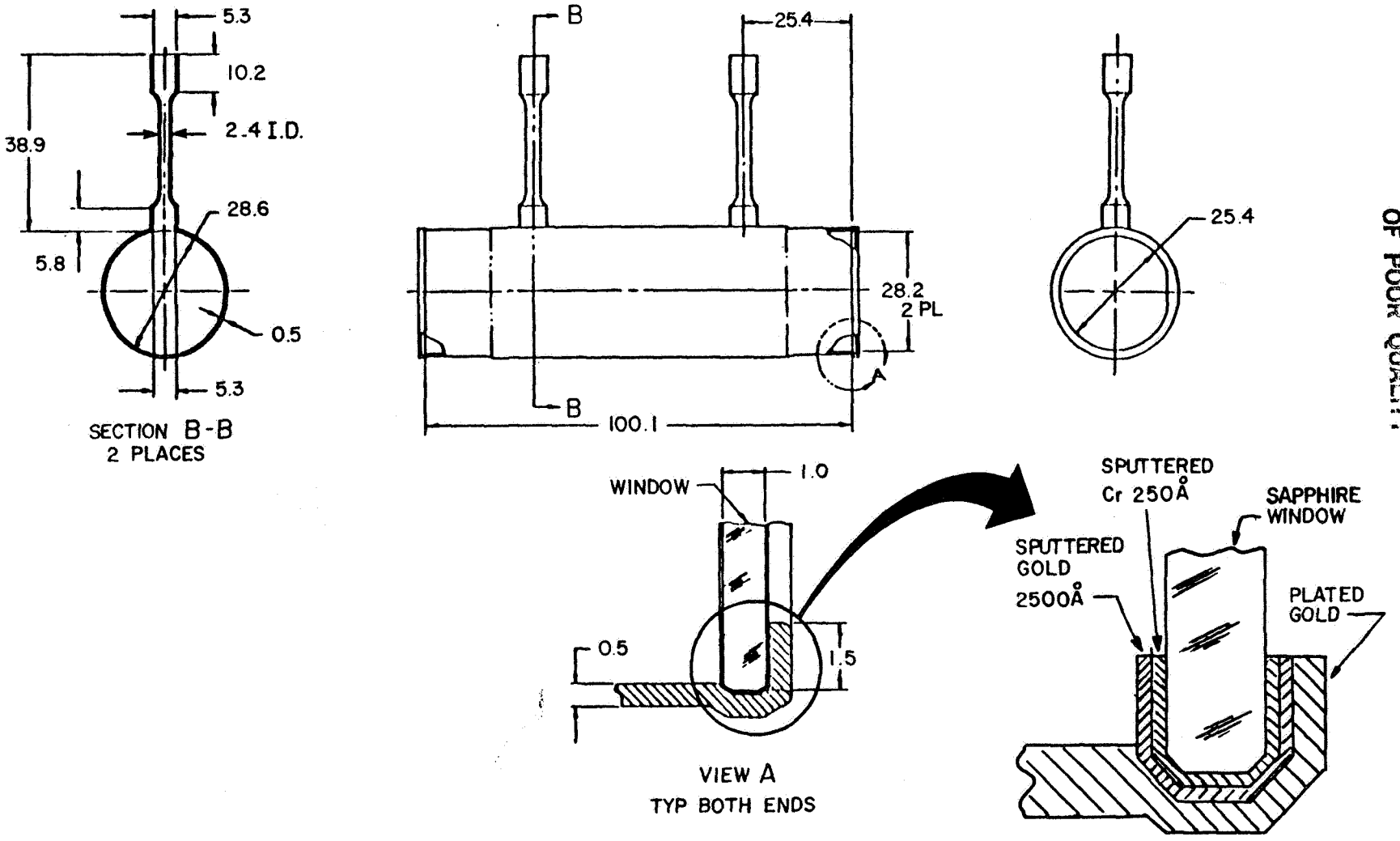

Figure 3.- Gold cell design. Dimensions are in millimeters.

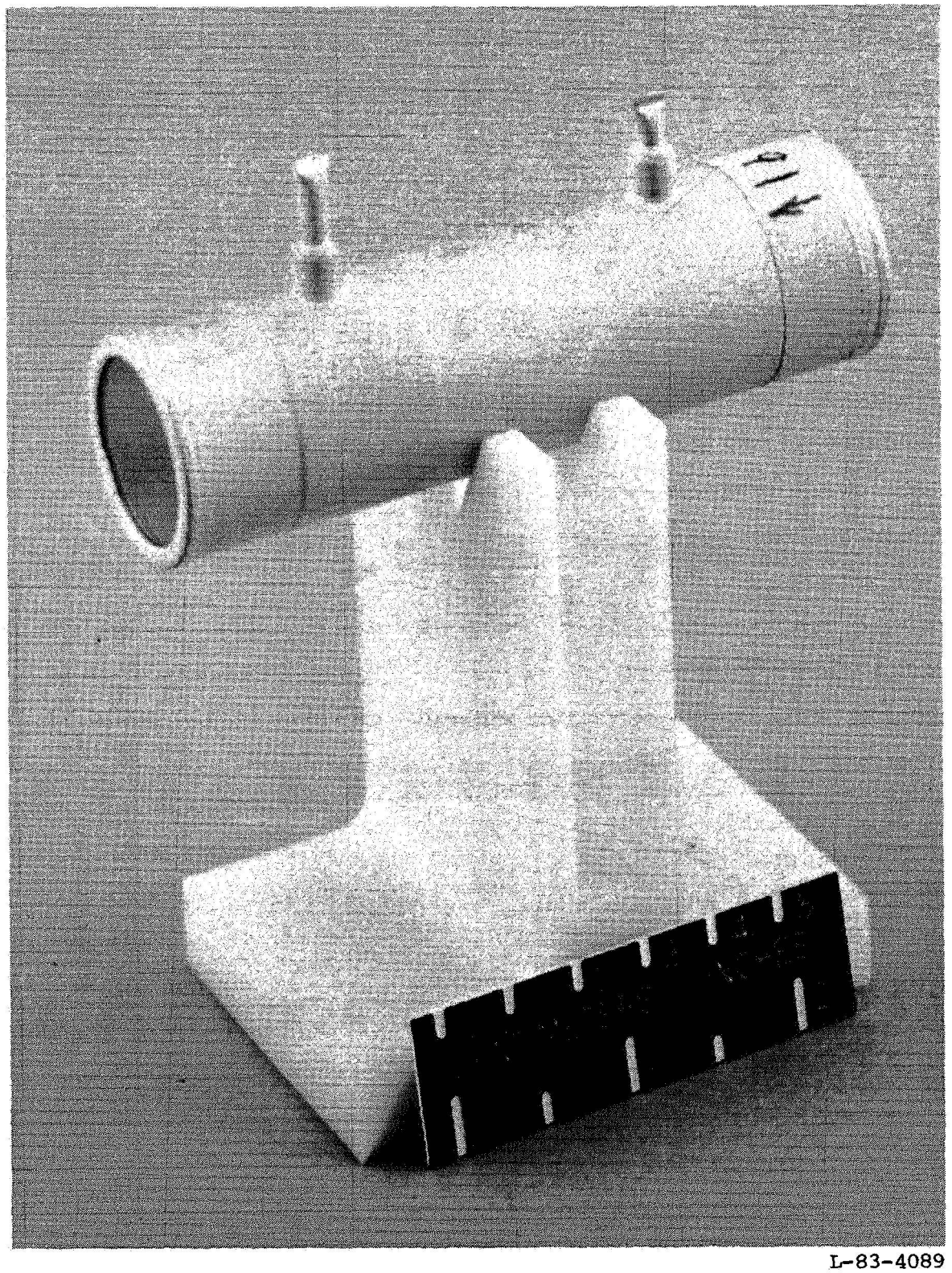

L-83-4089

Figure 4.- Gold cell.

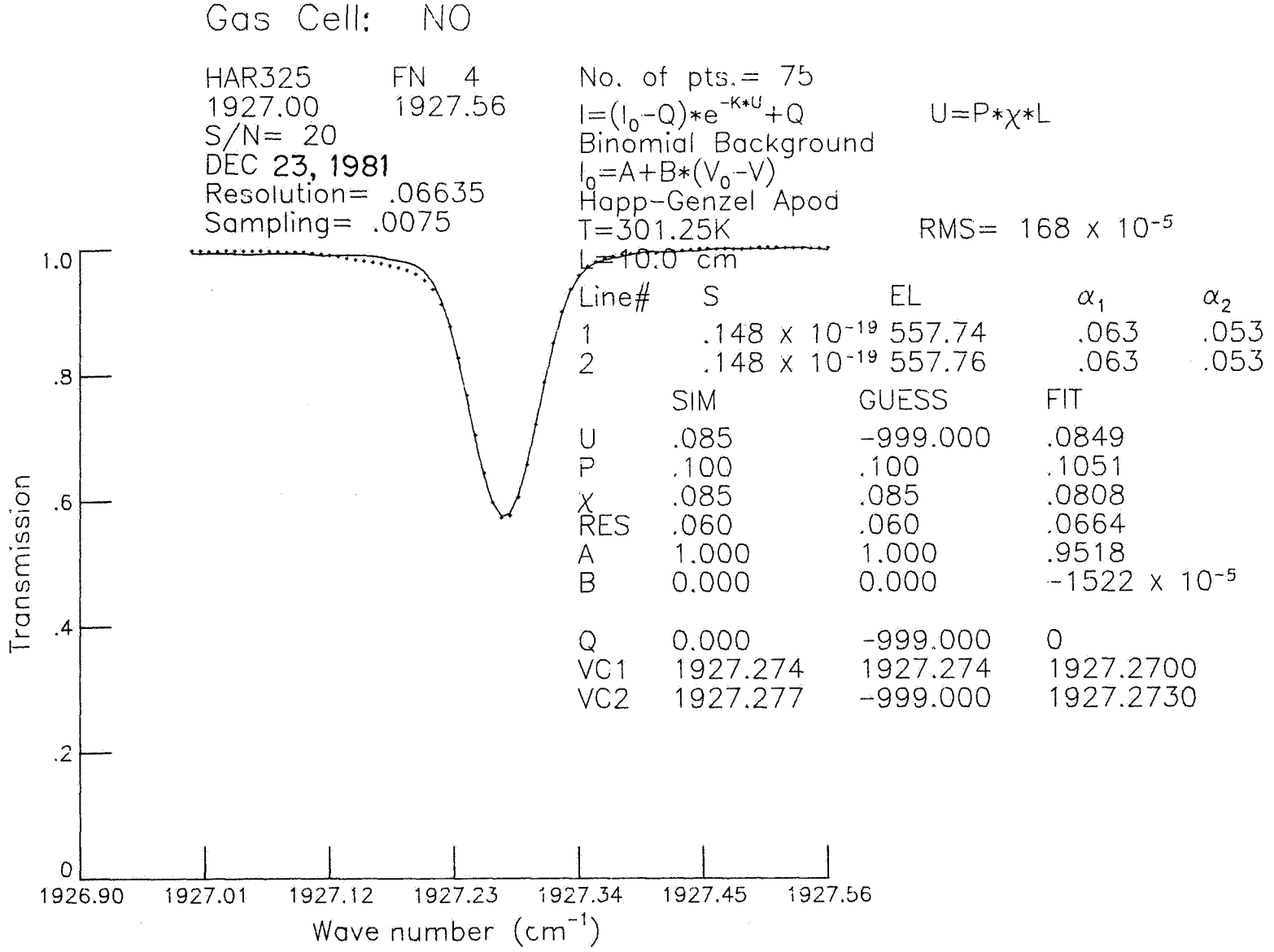

(a) Sample plot.

Figure 5.- Line fit plot for NO.

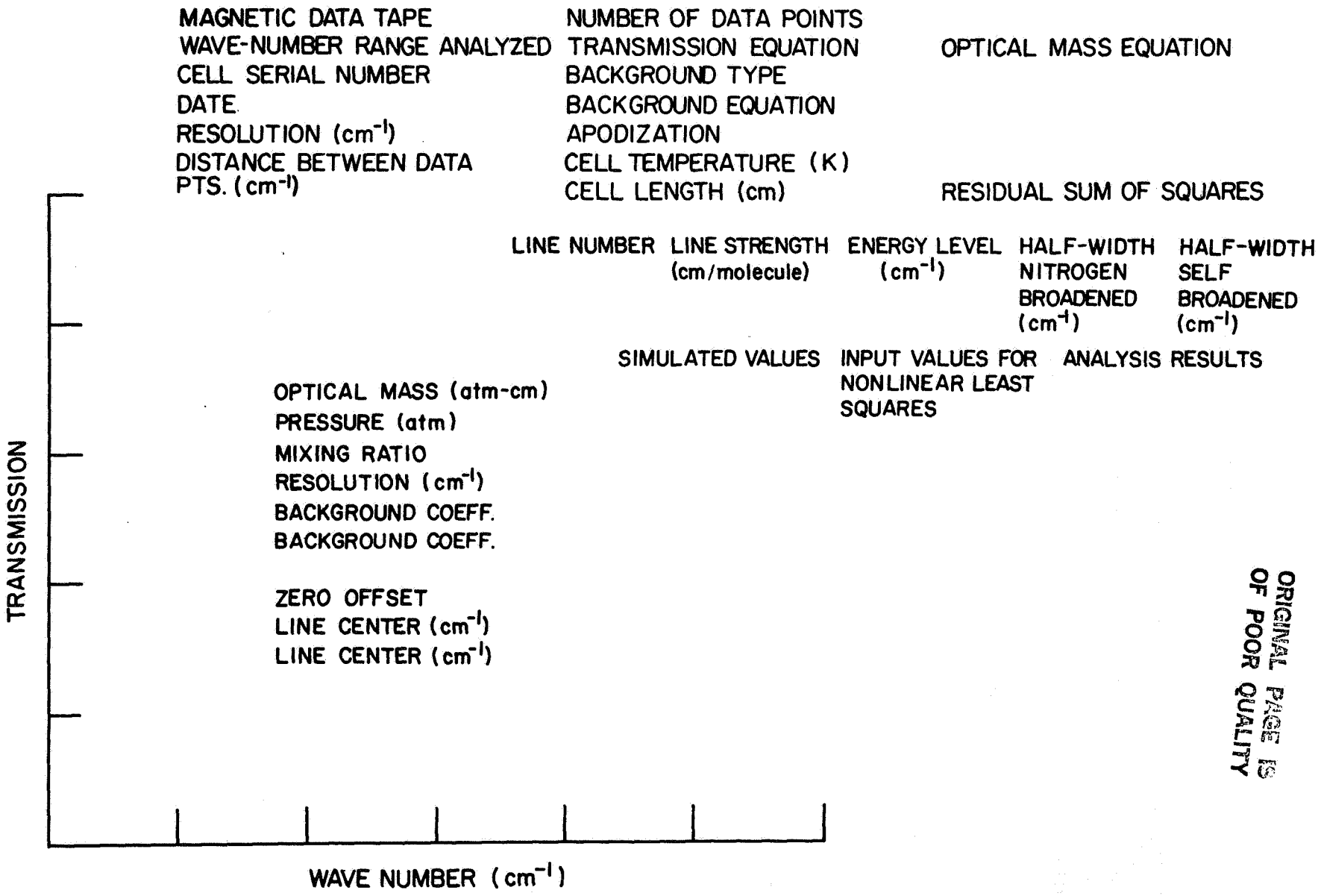

(b) Key to line fit plot.

Figure 5.- Continued.

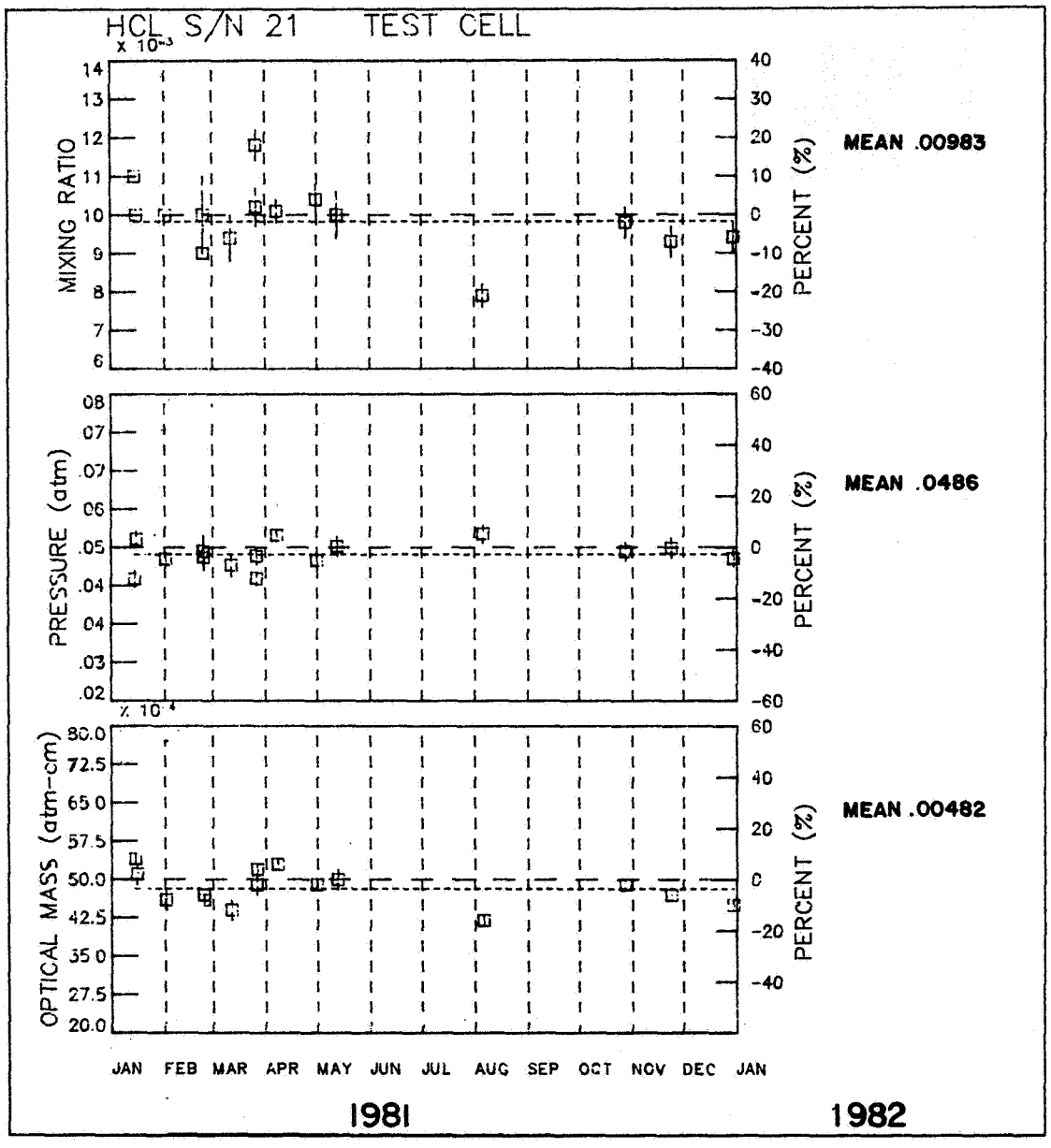

(c) Sample historical record (HCl cell S/N 21).

Figure 5.- Concluded.

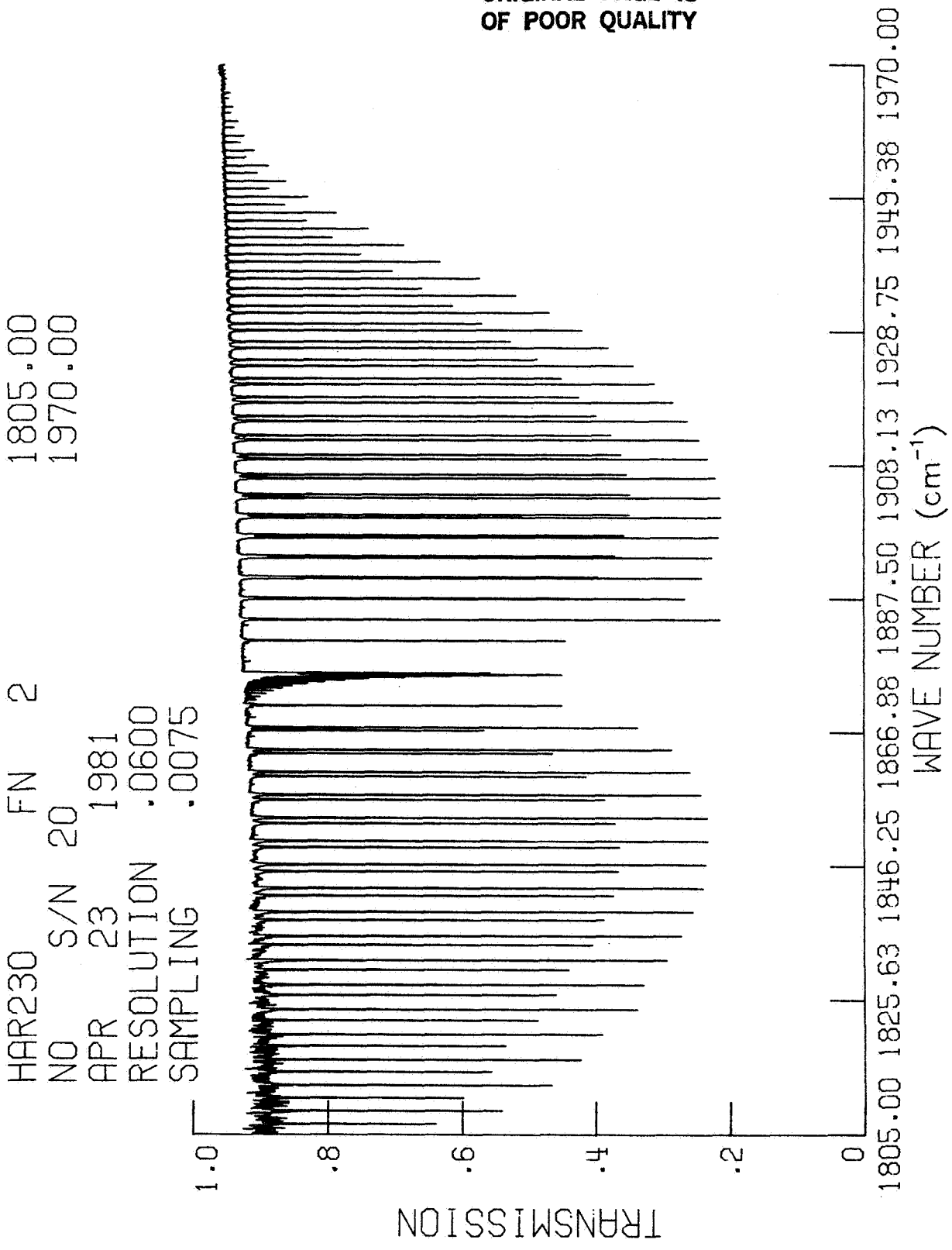

Figure 6.- Typical NO spectrum at ambient temperature.

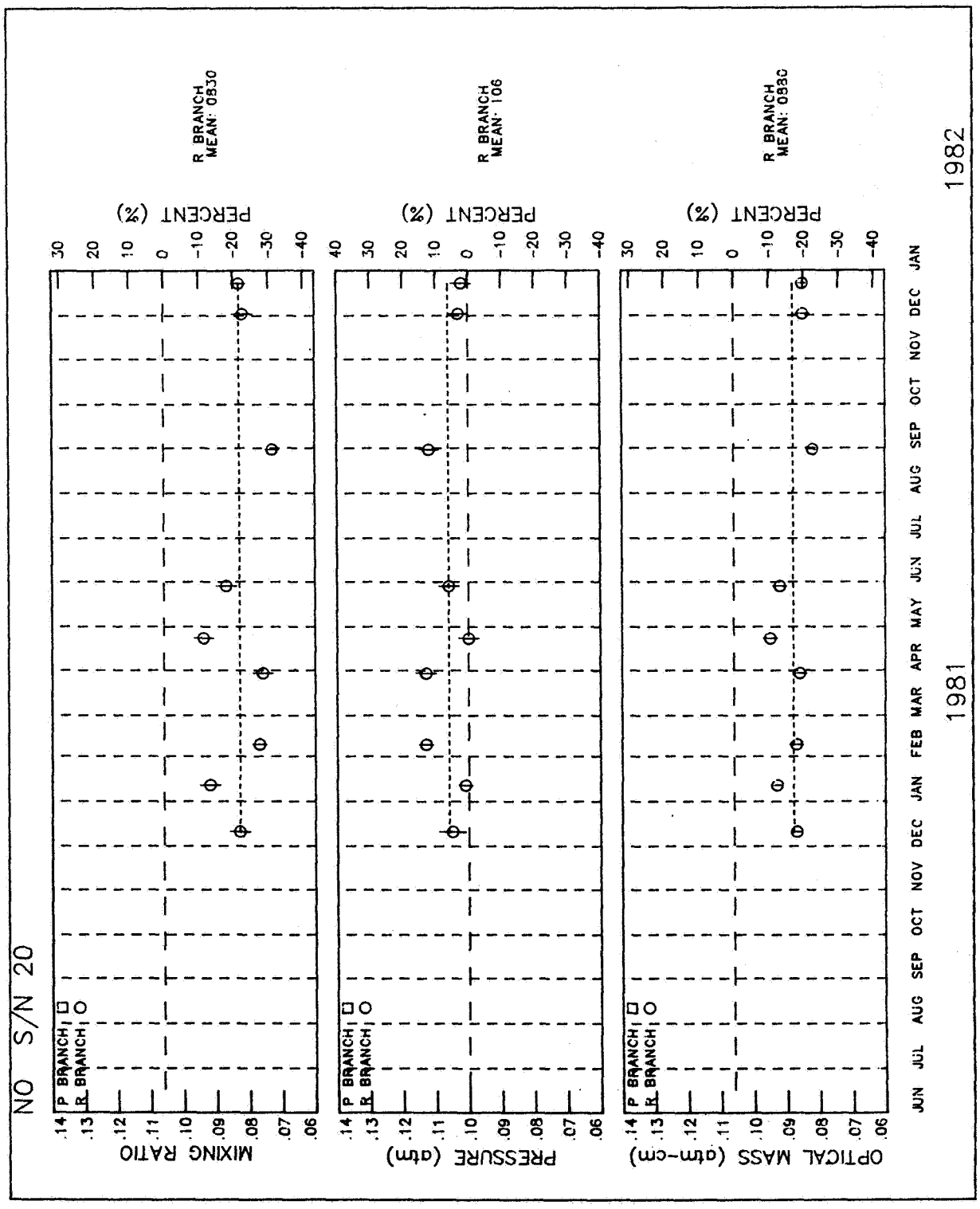

(a) S/N 20.

Figure 7.- Historical record for NO cells.

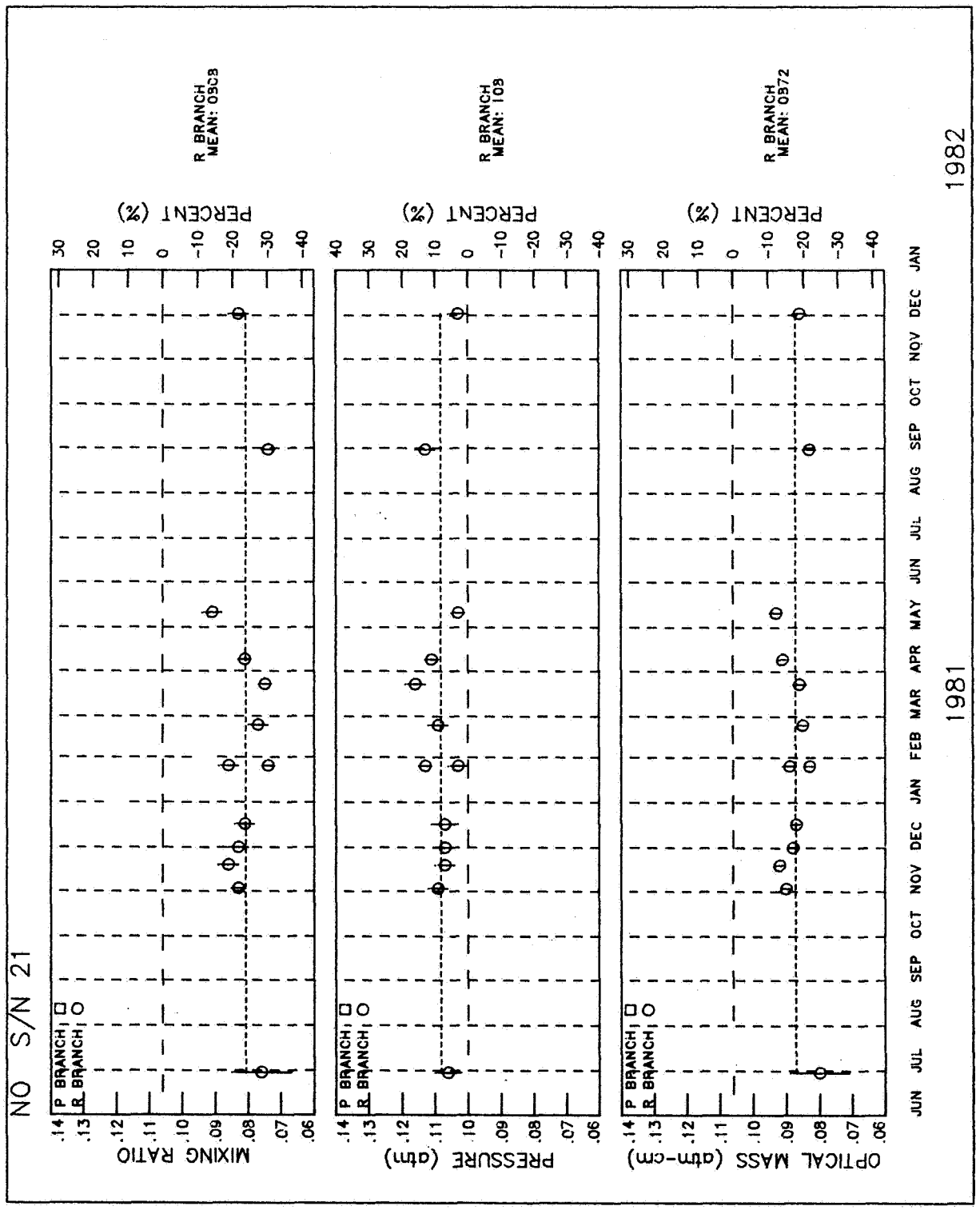

(b) S/N 21.

Figure 7.- Continued.

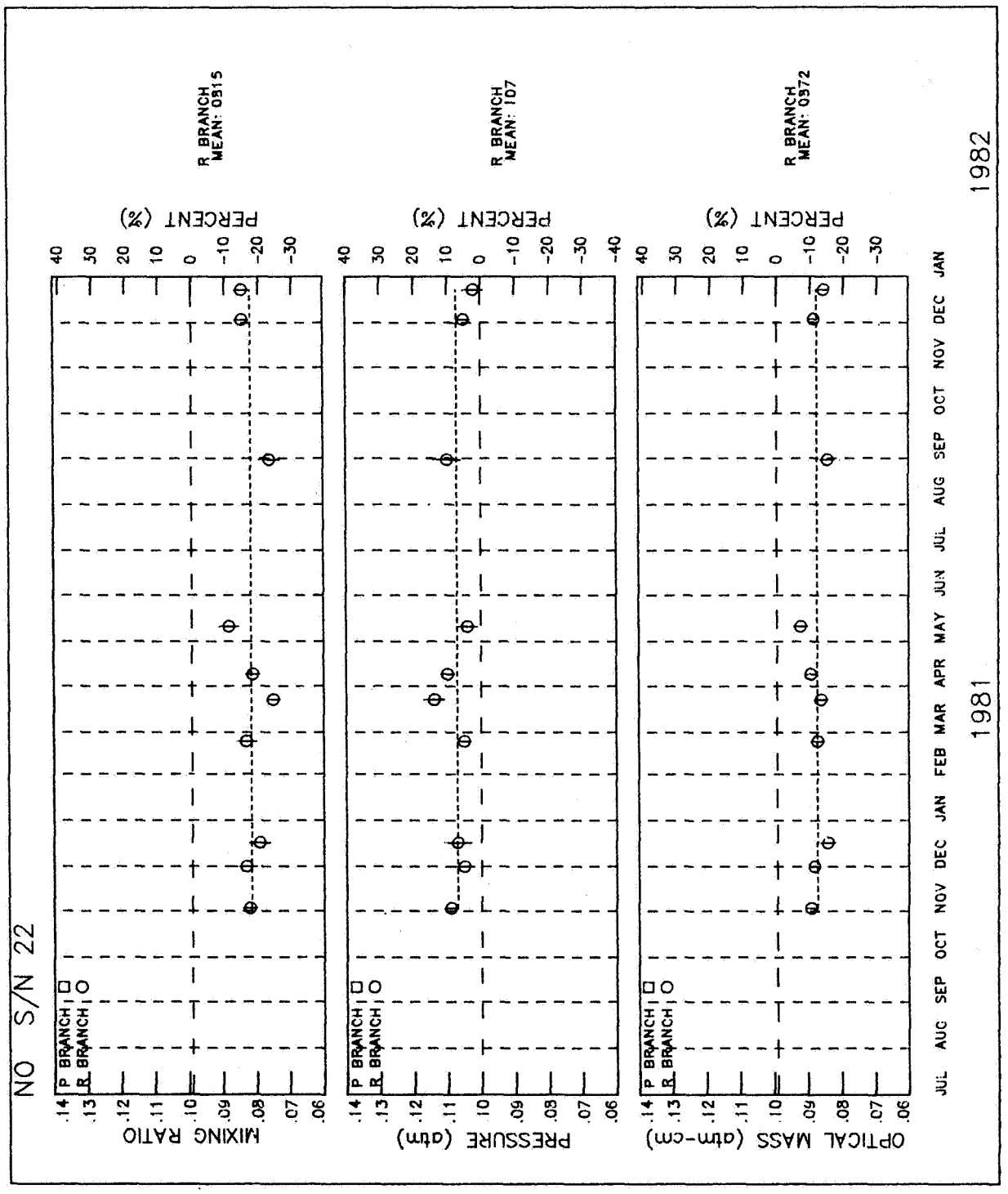

(c) S/N 22.

Figure 7.- Continued.

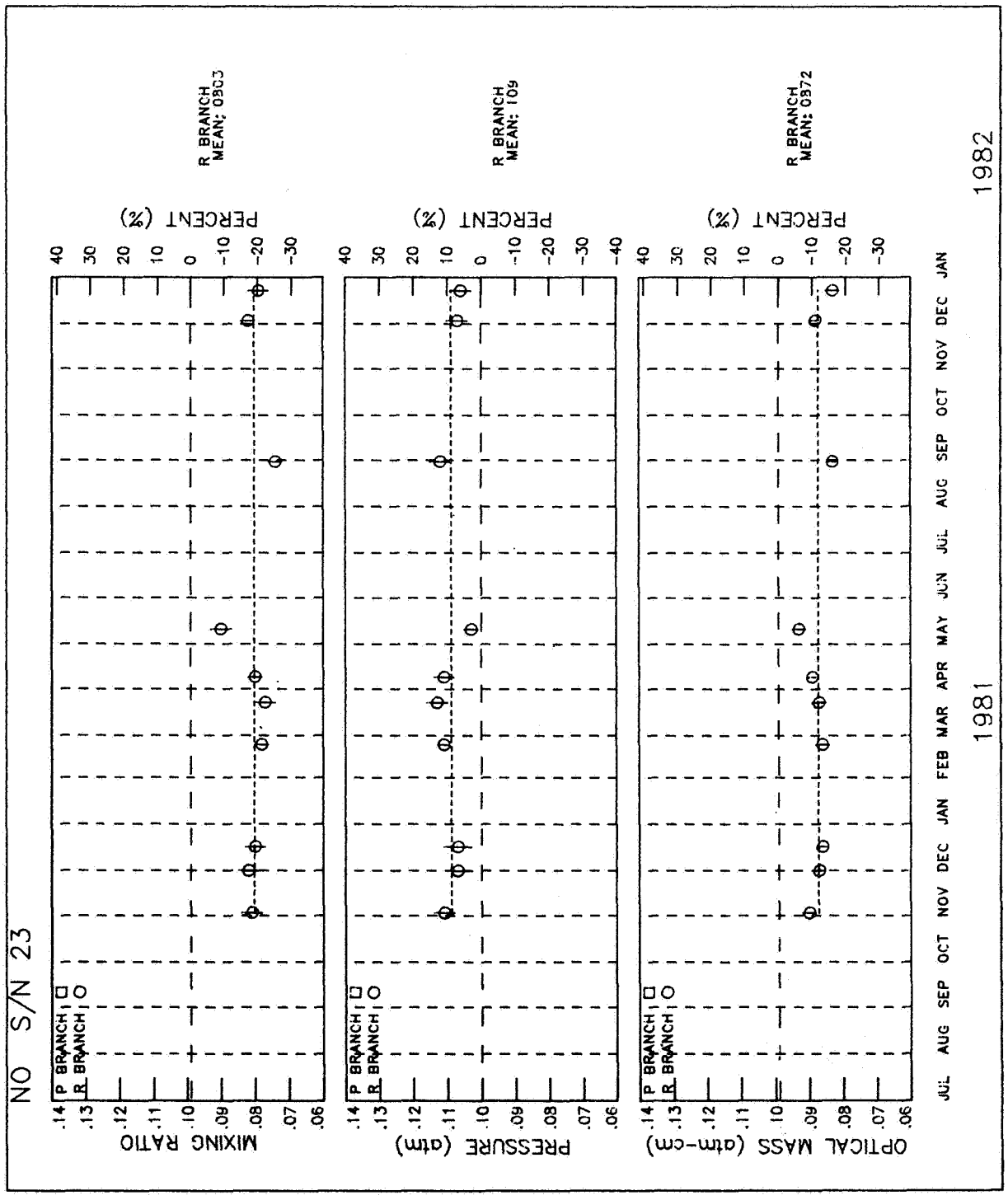

(d) S/N 23.

Figure 7.- Concluded.

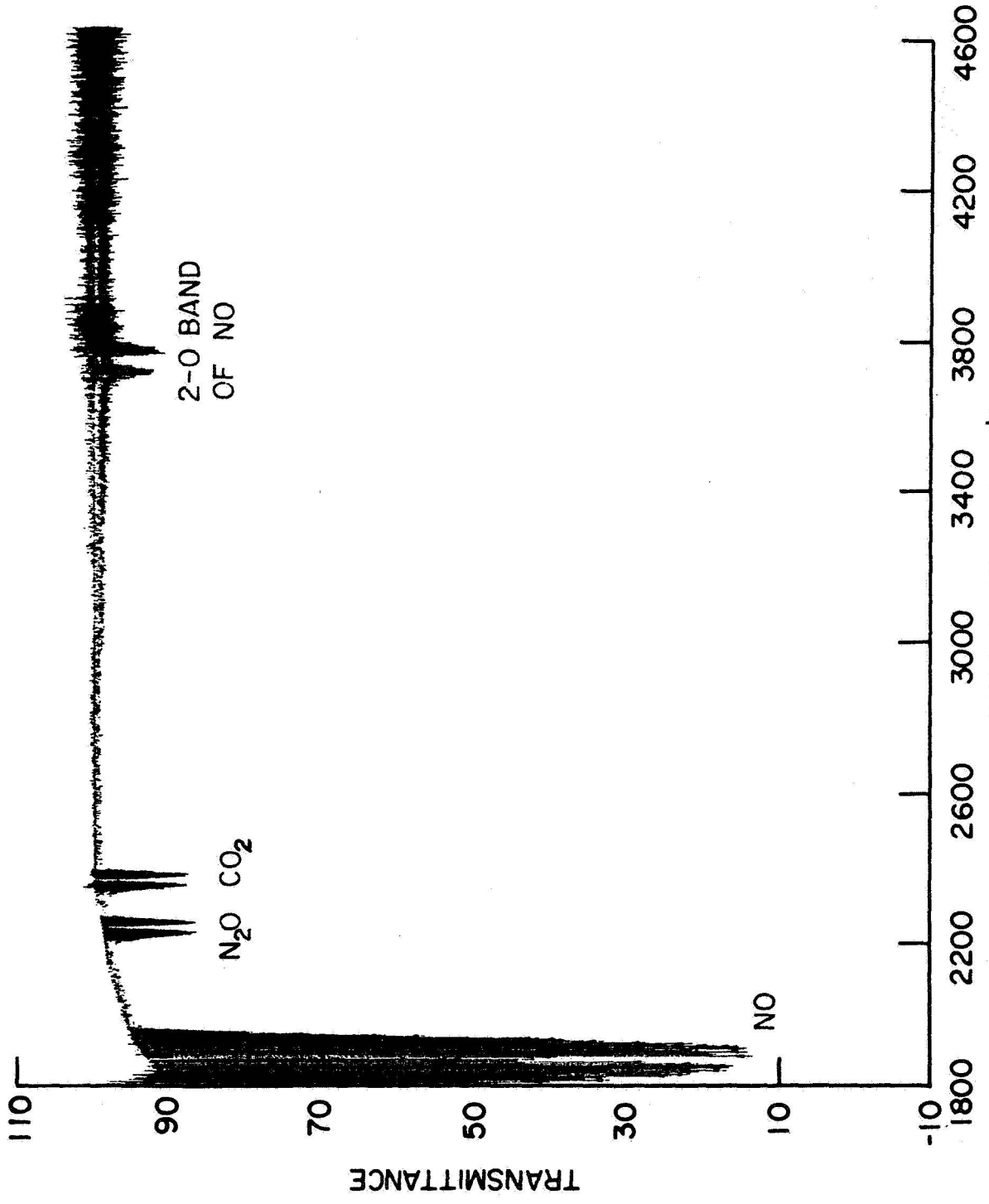

Figure 8.- Typical NO spectral survey.

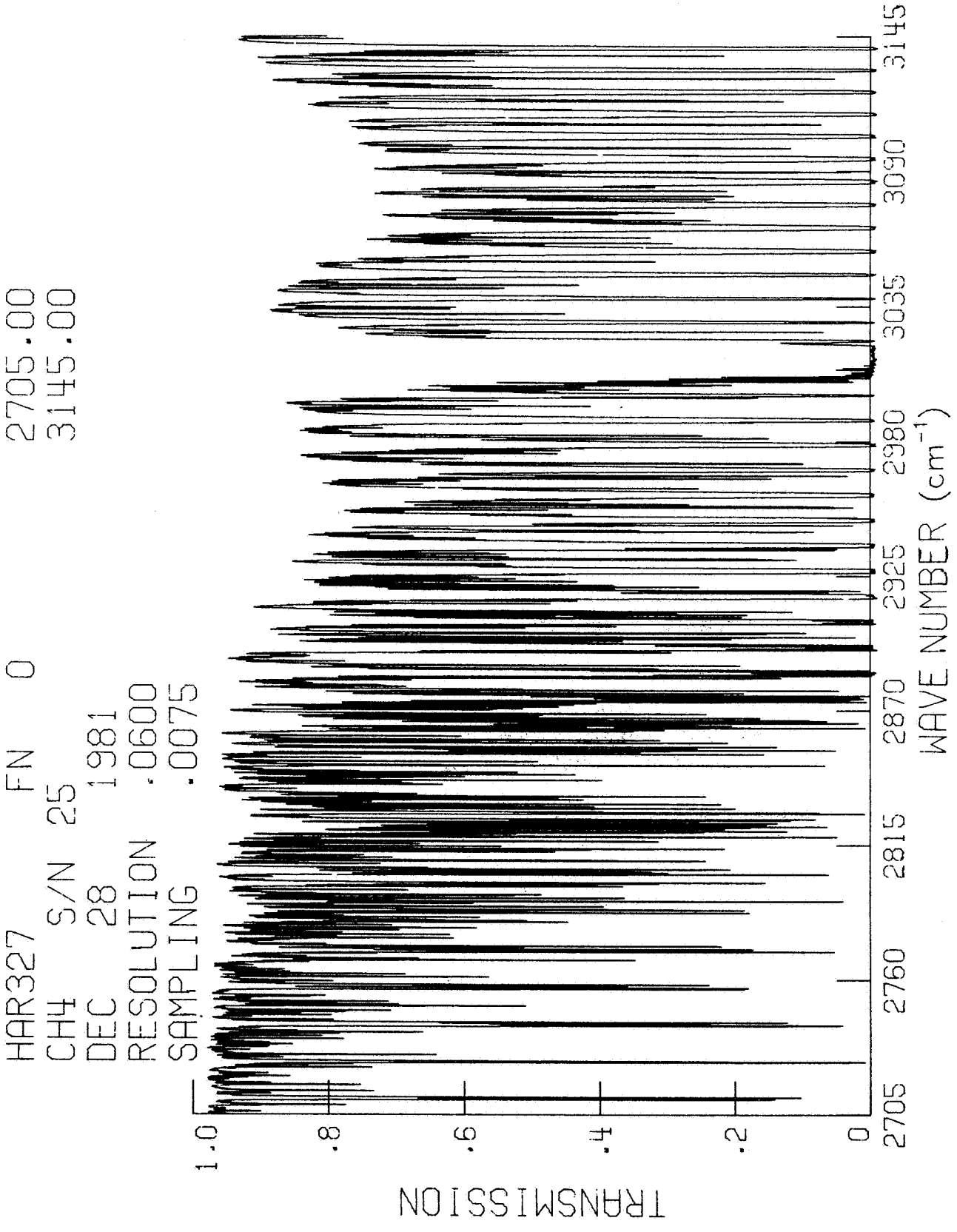

Figure 9.- Typical CH_4 spectrum at ambient temperature.

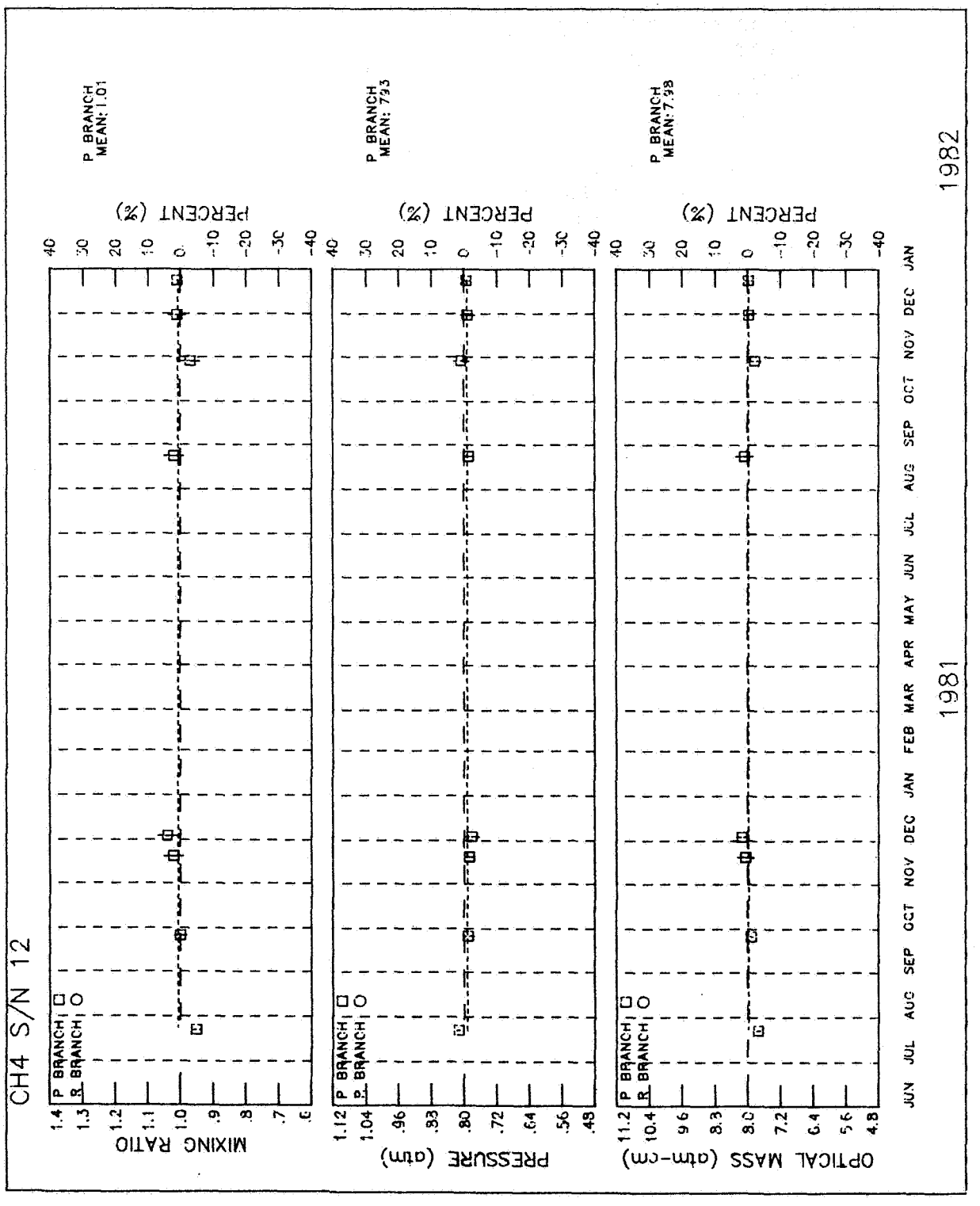

(a) S/N 12.

Figure 10.- Historical record for CH_4 cells.

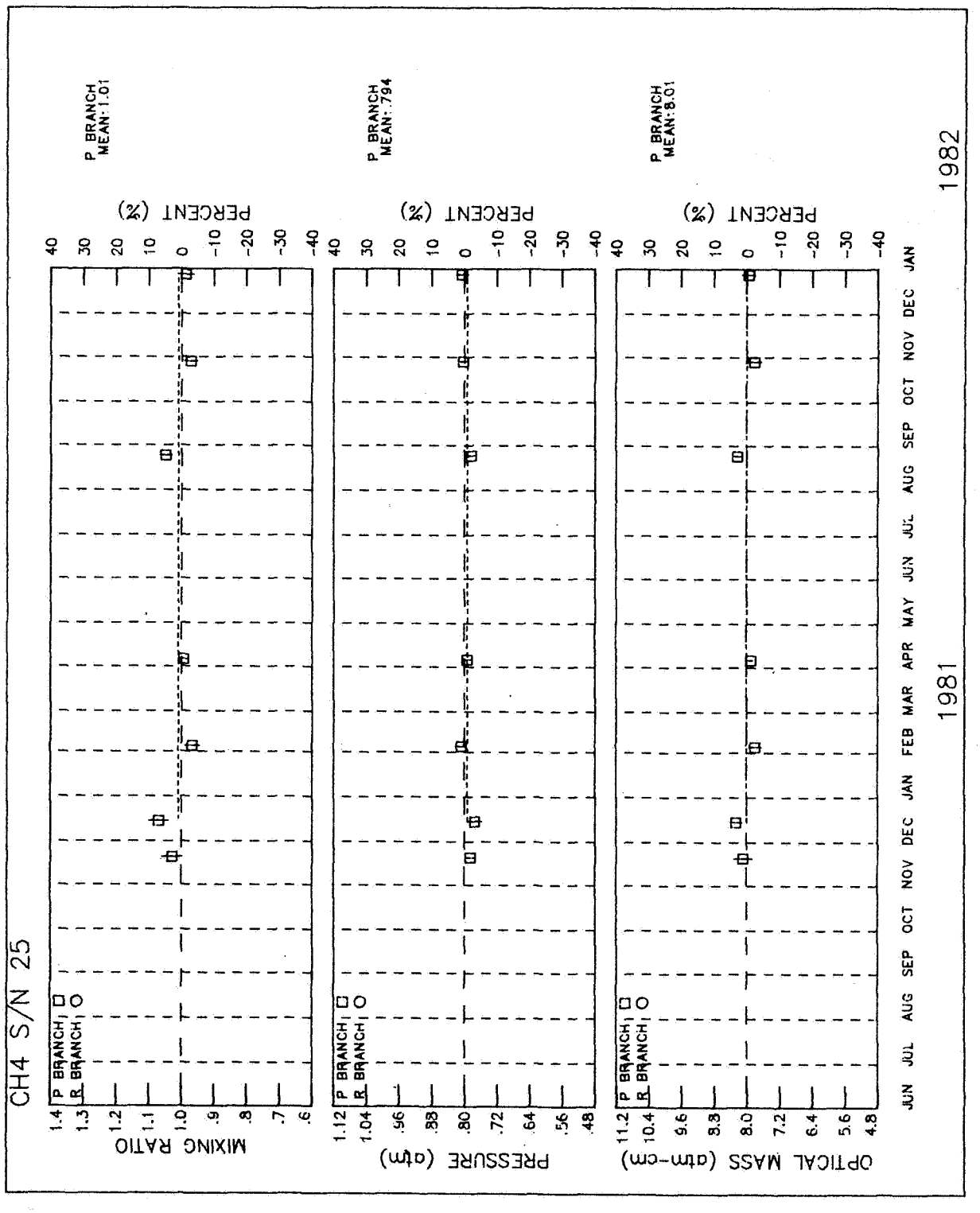

(b) S/N 25.

Figure 10.- Continued.

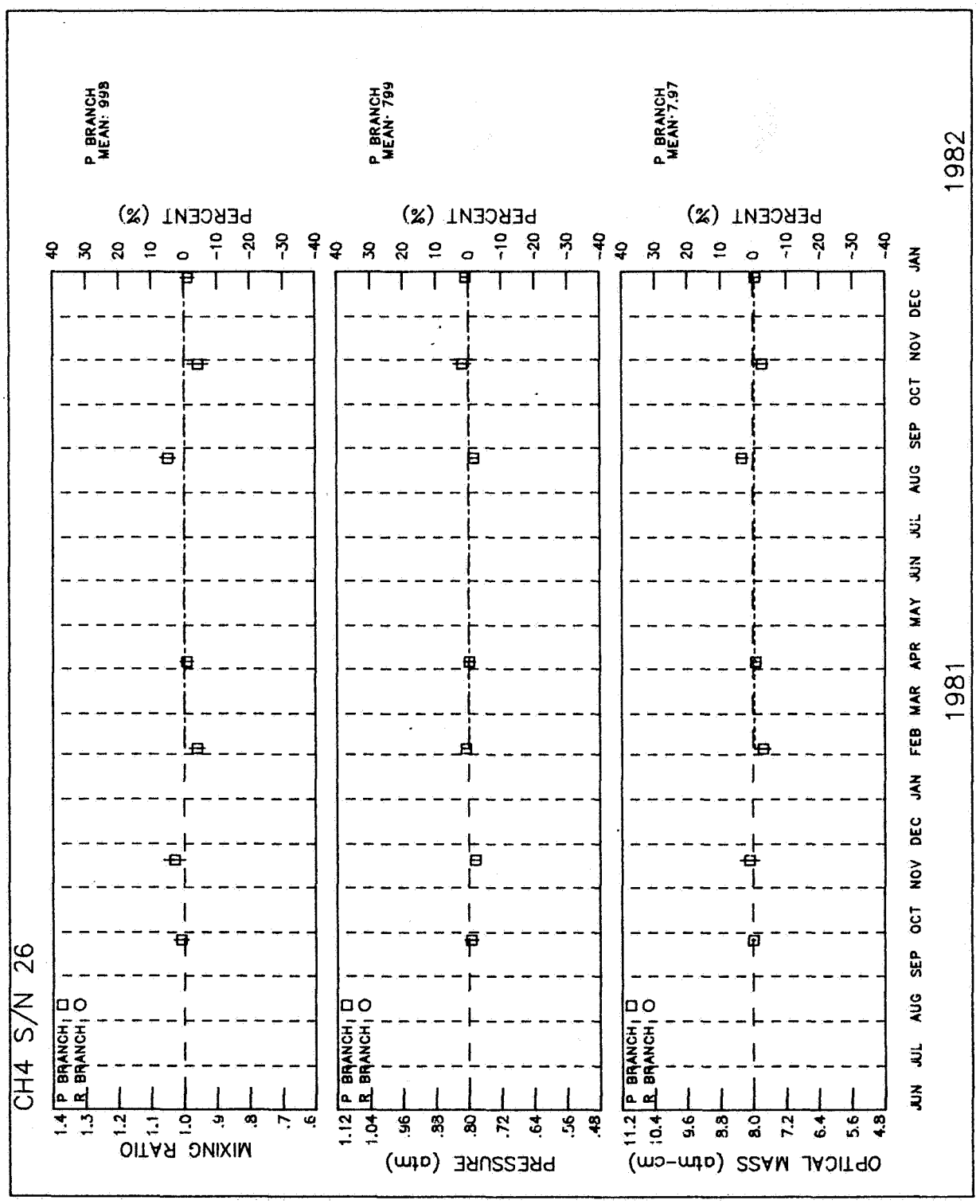

(c) S/N 26.

Figure 10.- Concluded.

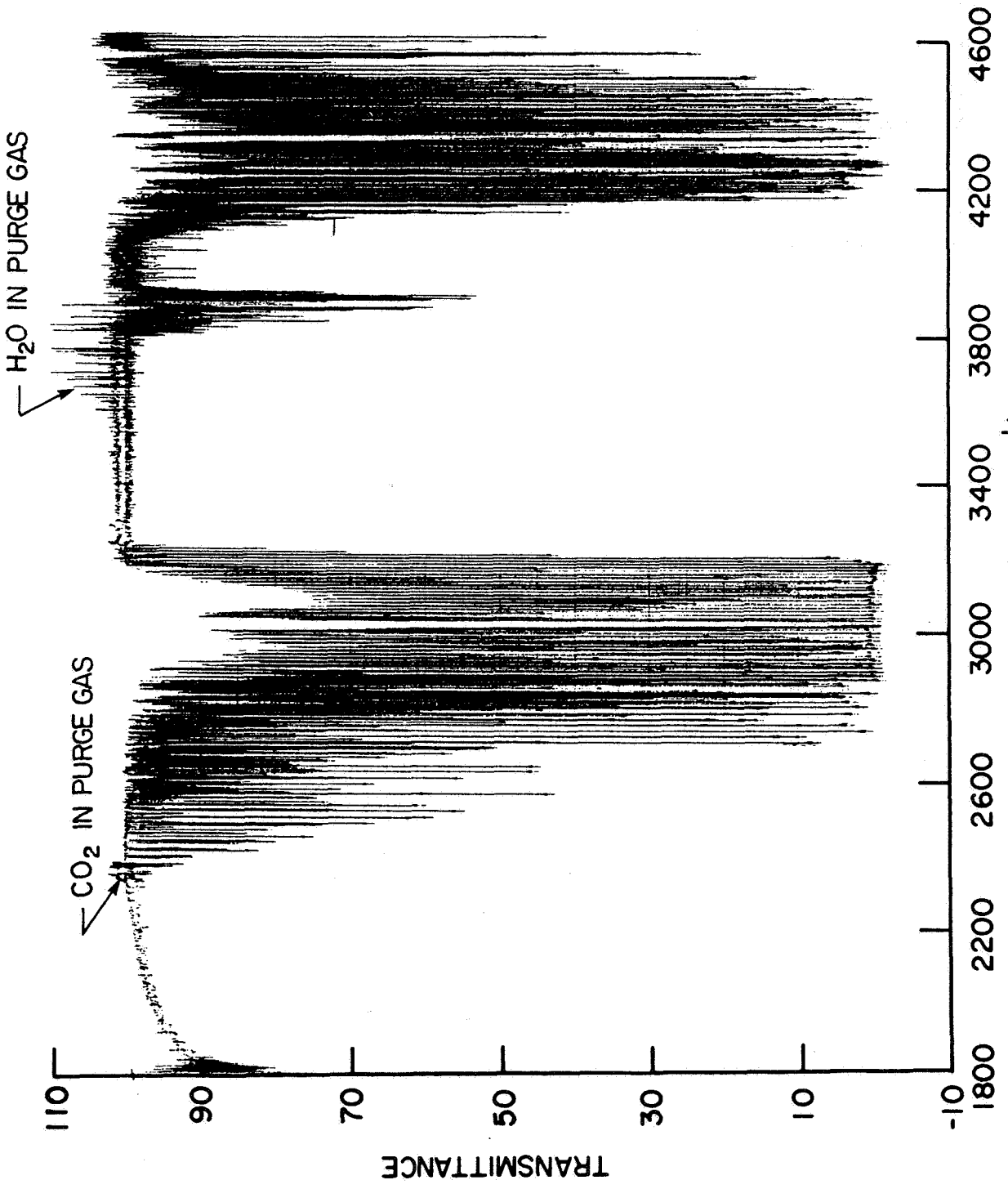

Figure 11.- Typical CH_4 spectral survey.

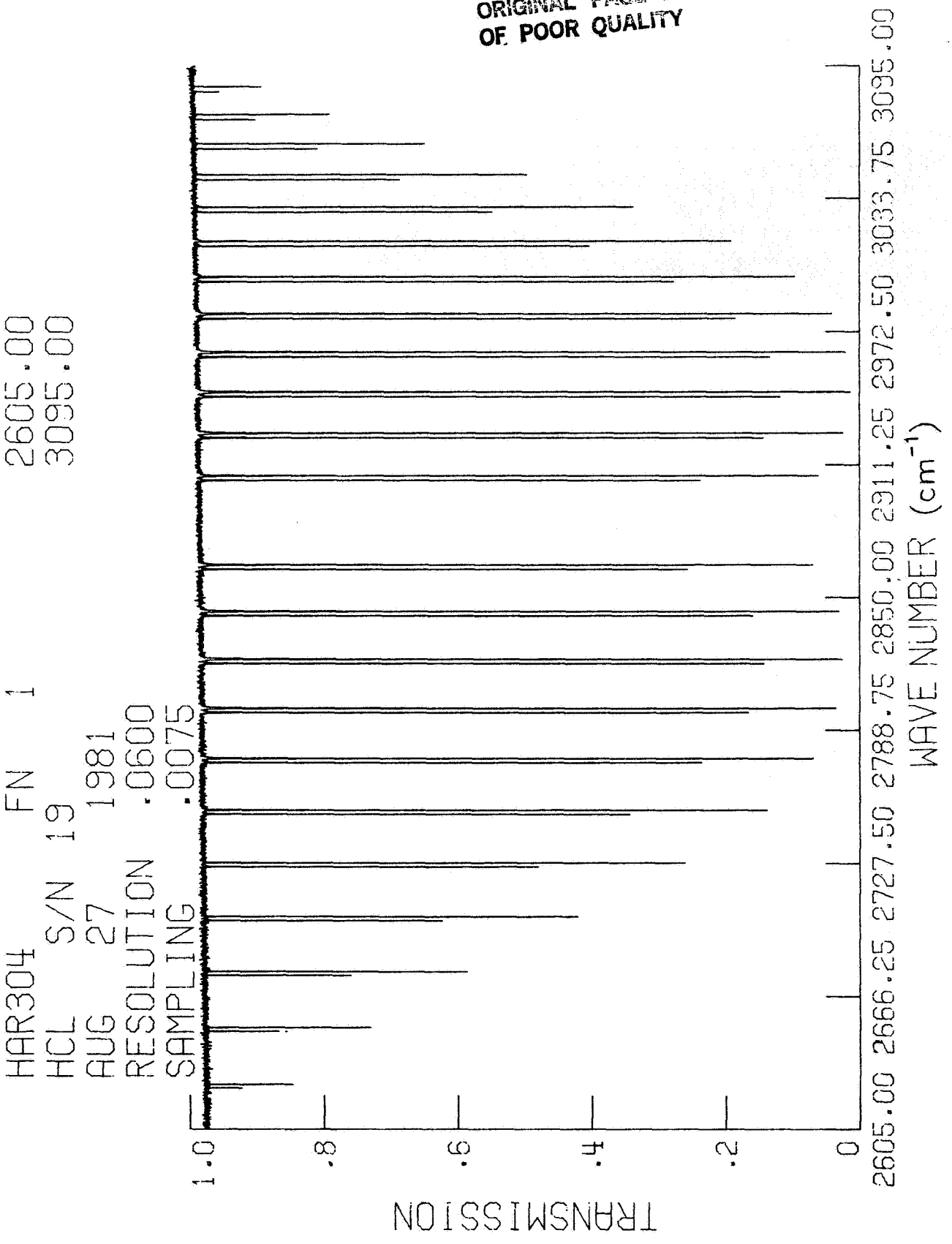

Figure 12.- Typical HCl spectrum at ambient temperature.

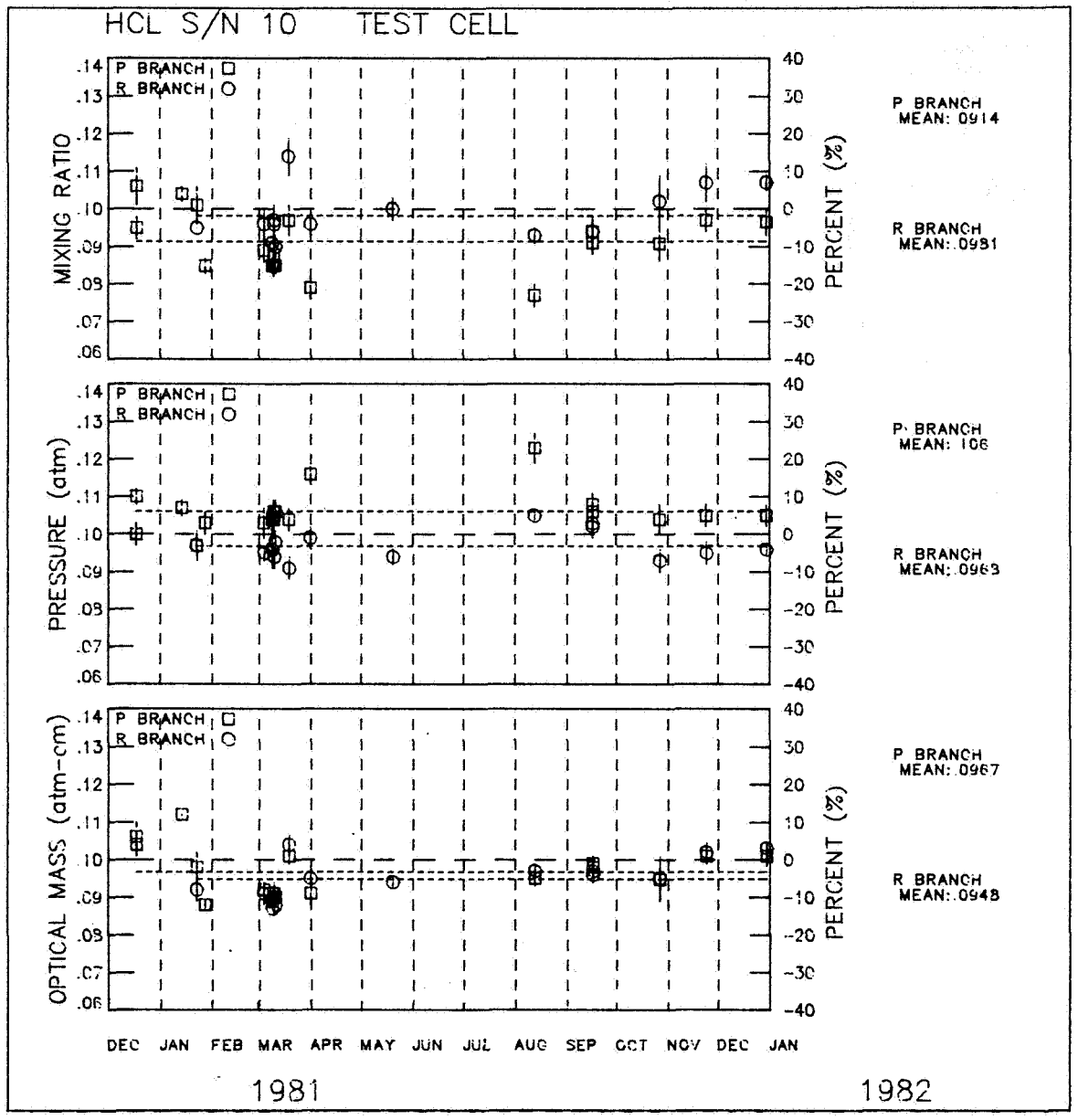

(a) S/N 10.

Figure 13.- Historical record for HCl cells.

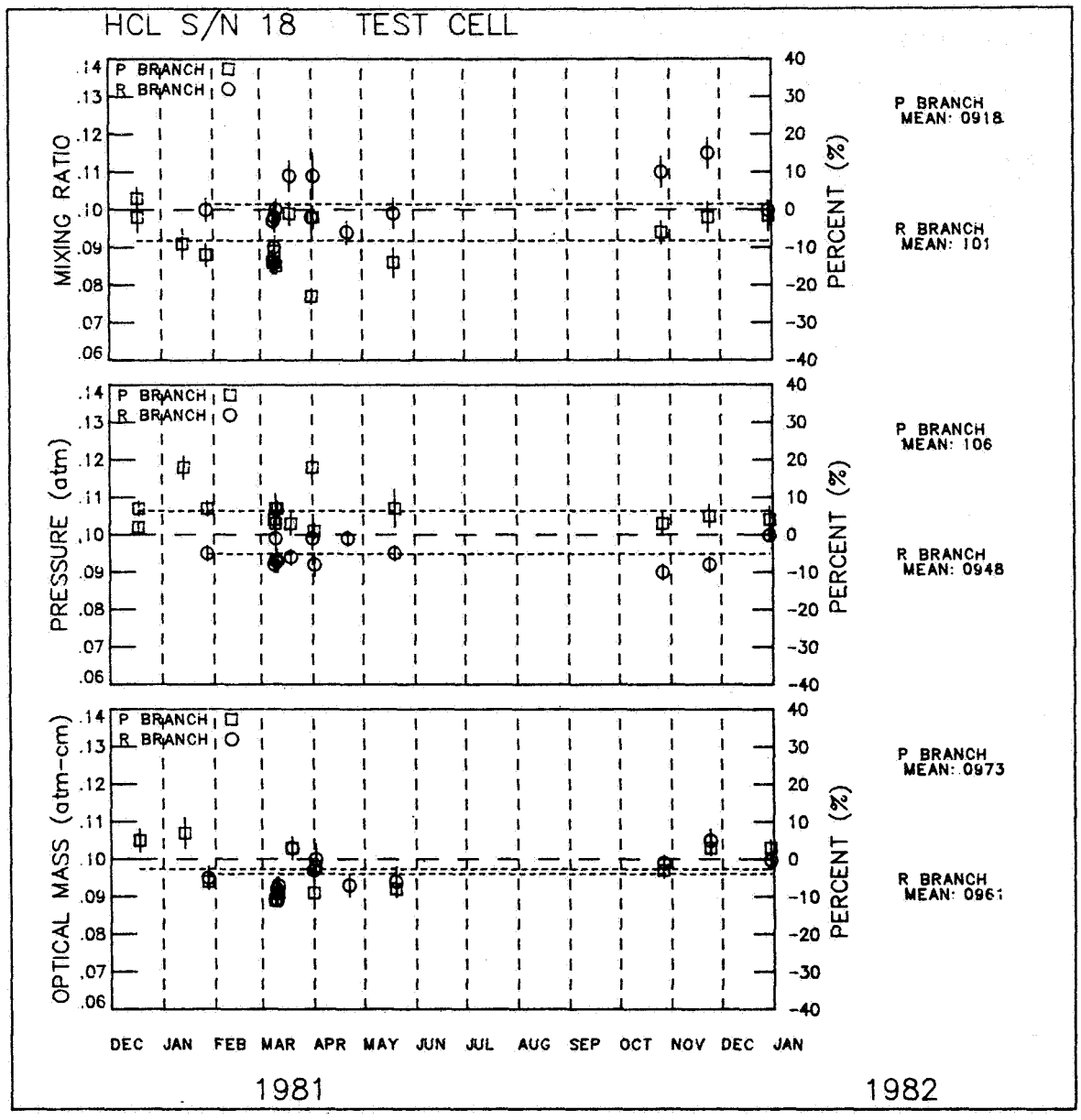

(b) S/N 18.

Figure 13.- Continued.

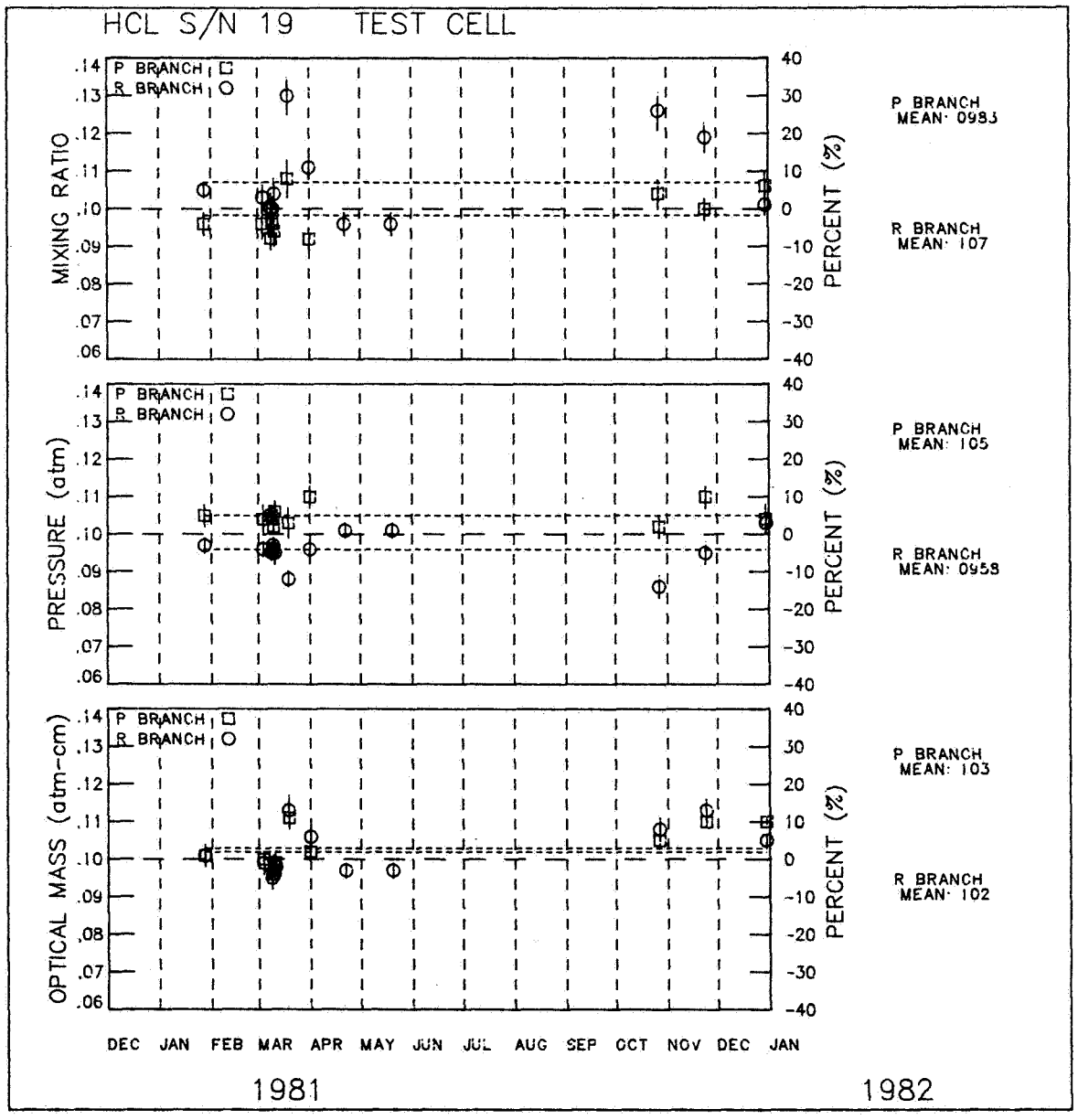

(c) S/N 19.

Figure 13.- Continued.

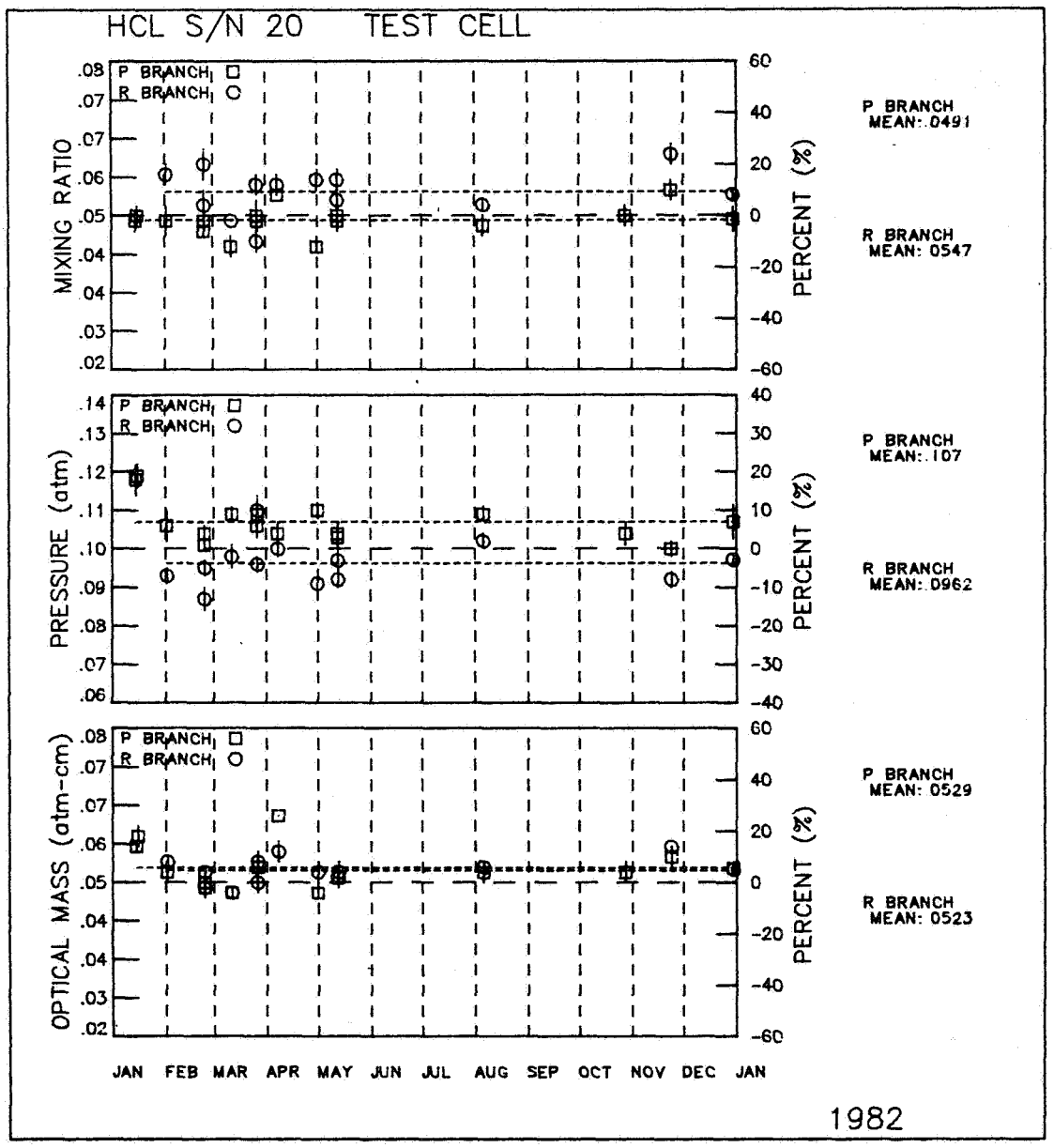

(d) S/N 20.

Figure 13.- Concluded.

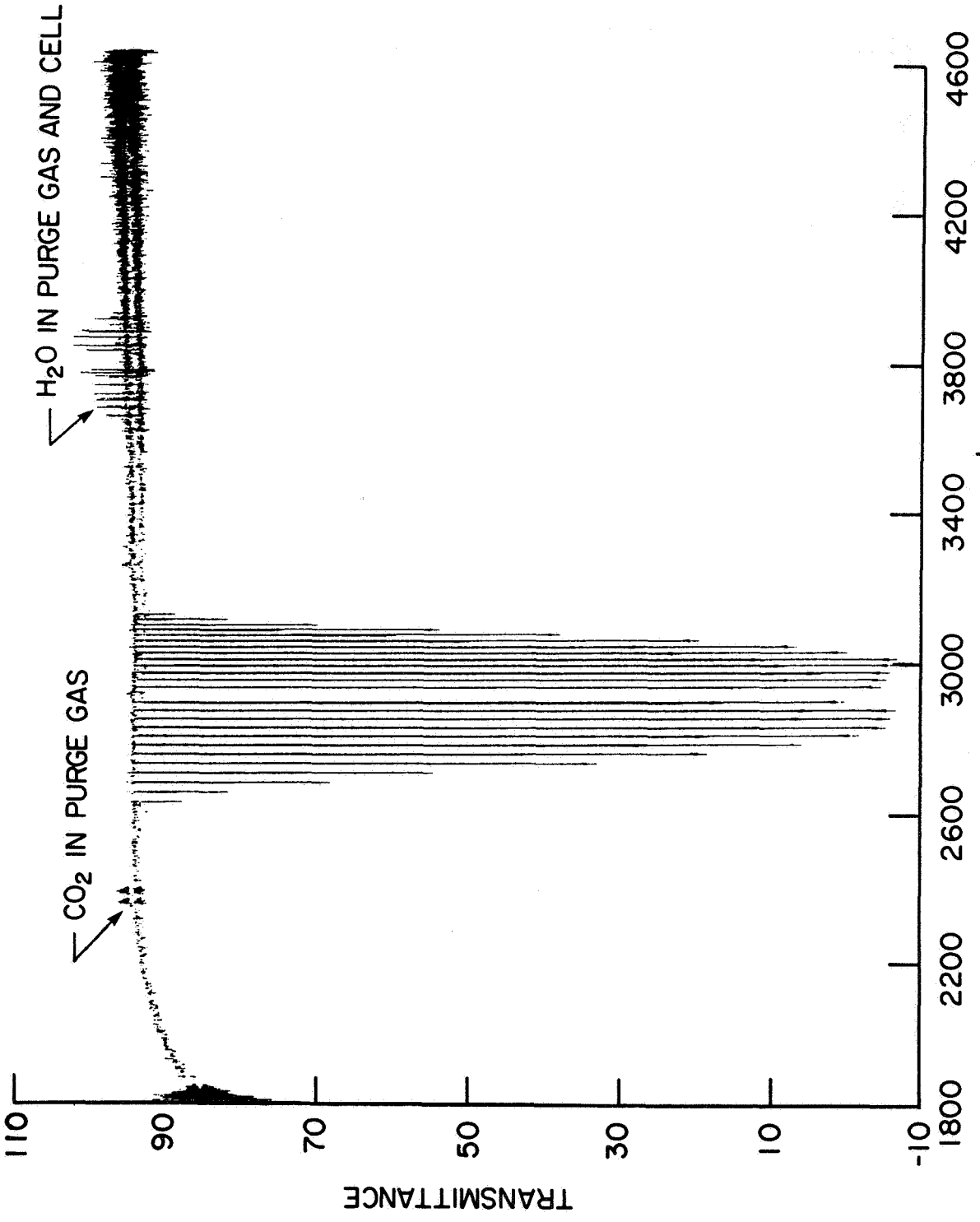

Figure 14.- Spectral survey for HCl cell S/N 18.

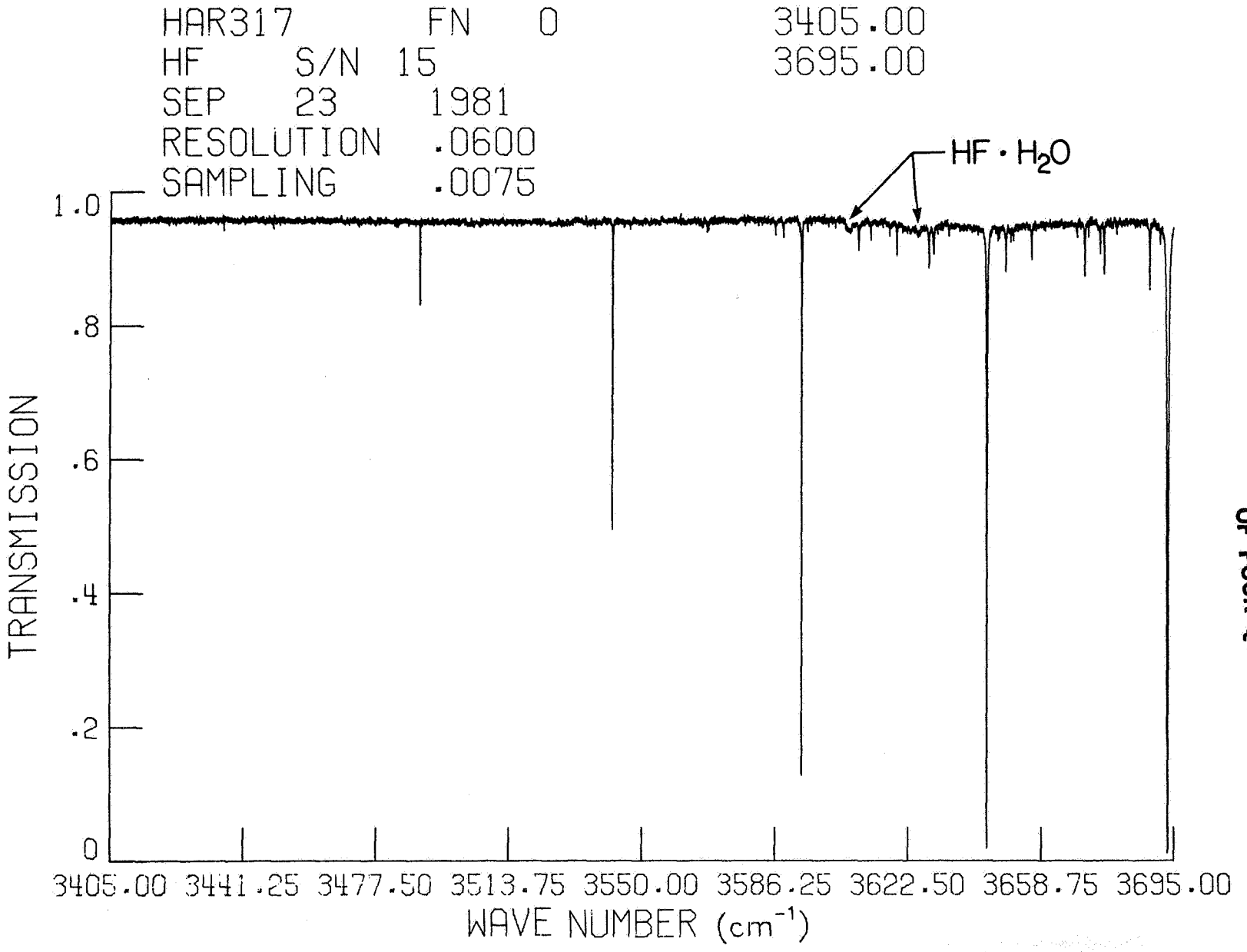

(a) P branch.

Figure 15.- HF spectrum at ambient temperature for cell S/N 15.

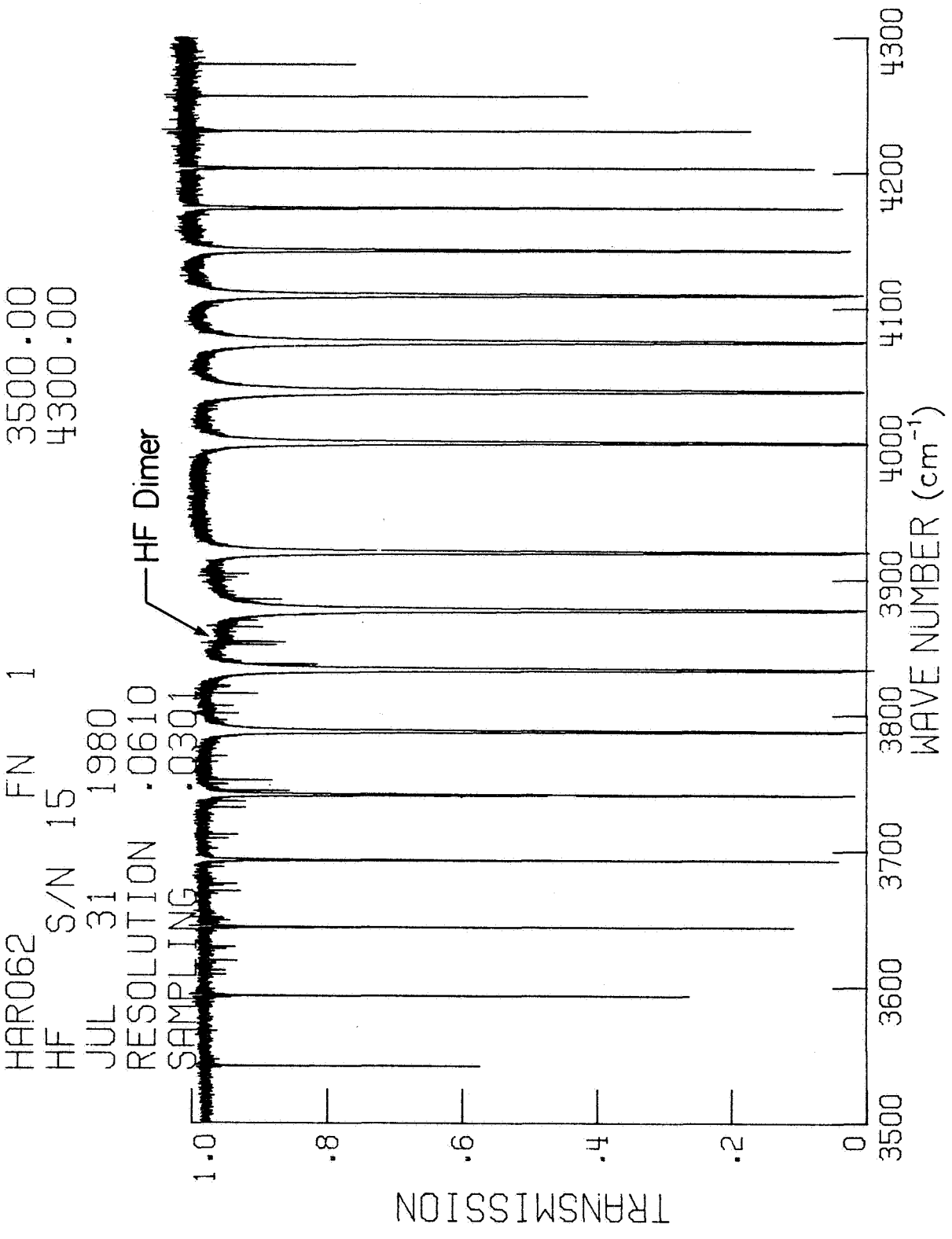

(b) P and R branches.

Figure 15.- Concluded.

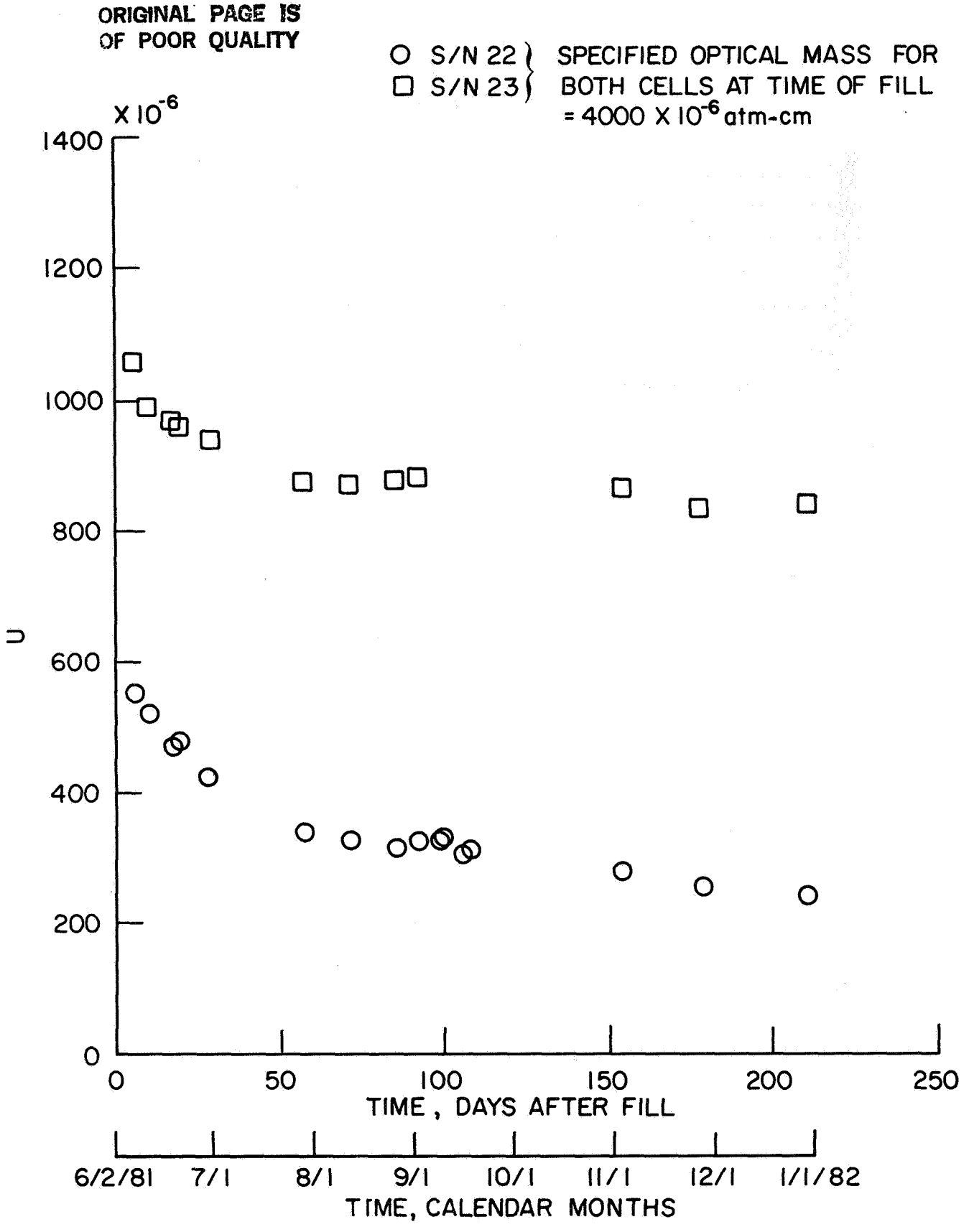

Figure 16.- Decay of optical mass in cells S/N 22 and S/N 23.

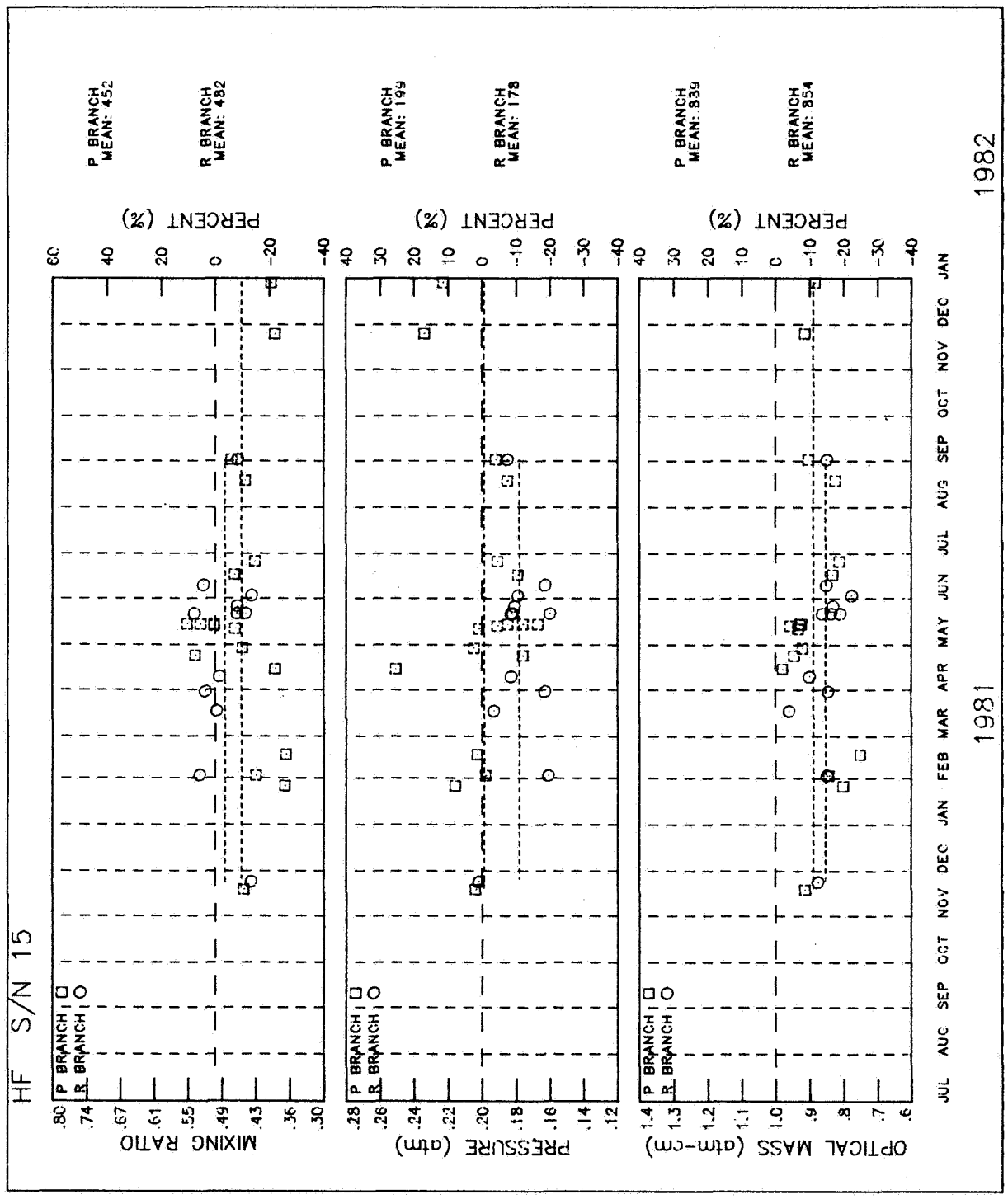

(a) S/N 15.

Figure 17.- Historical record for HF cells.

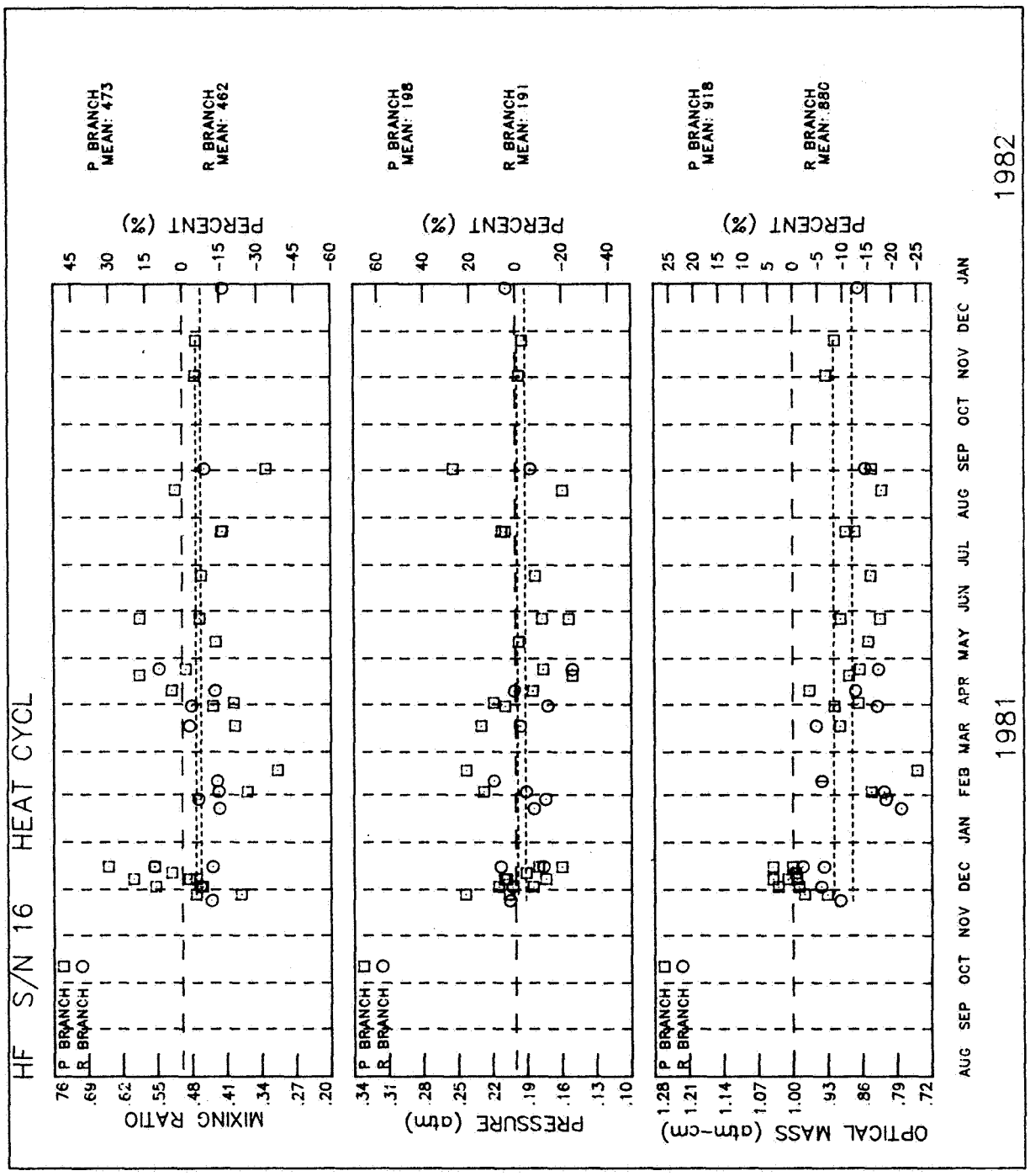

(b) S/N 16.

Figure 17.- Continued.

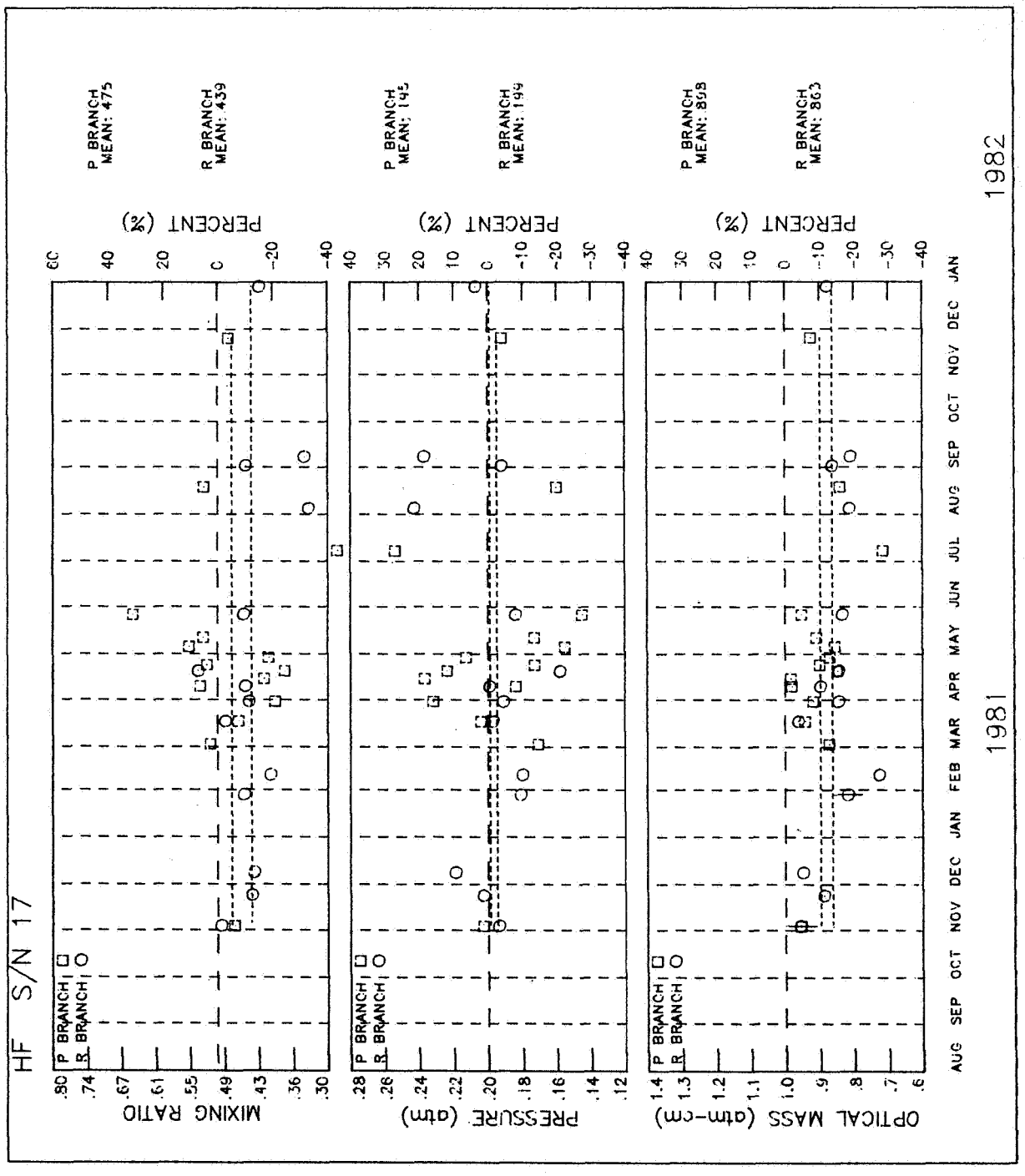

(c) S/N 17.

Figure 17.- Concluded.

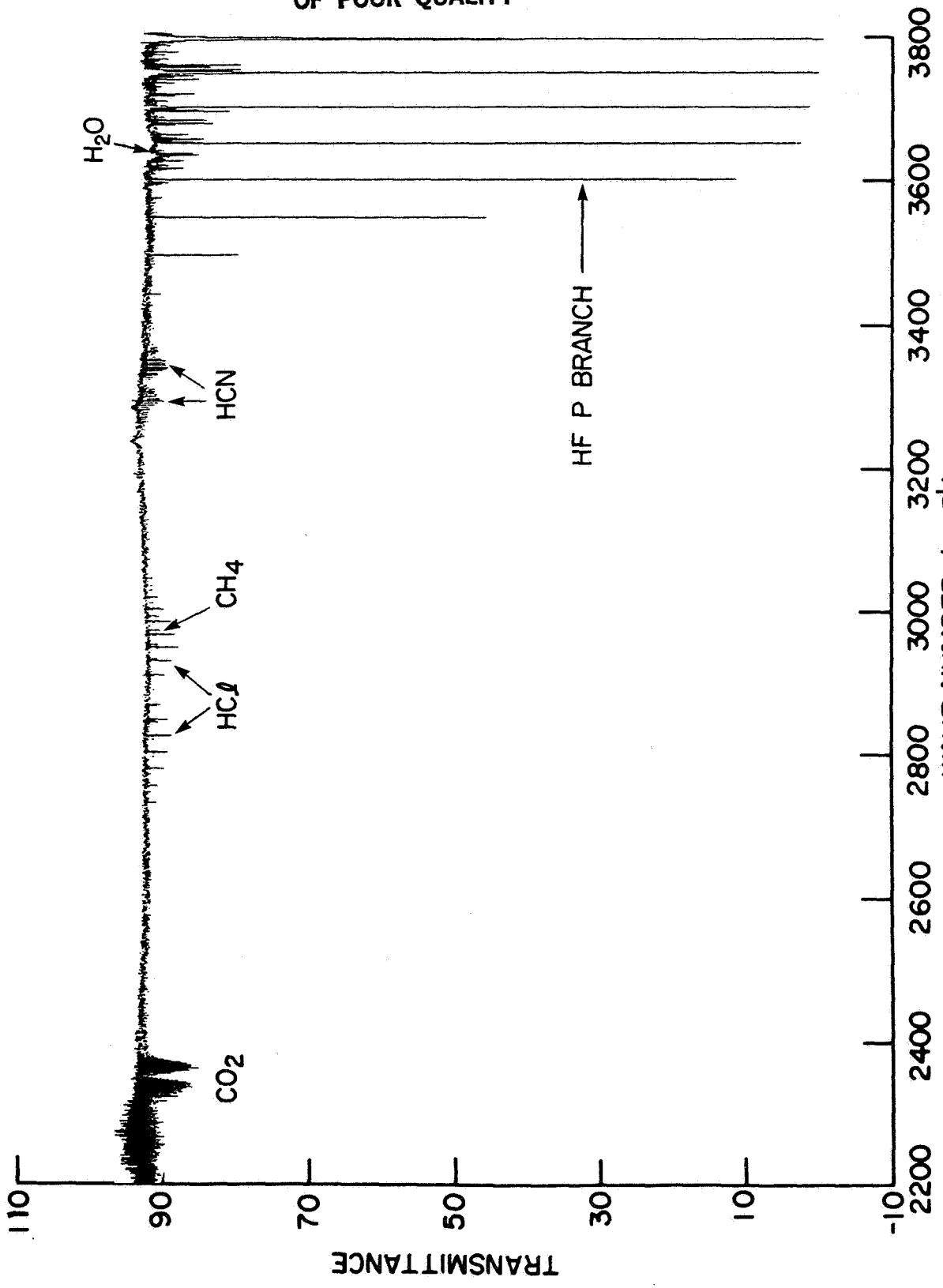

Figure 18.- Survey spectrum for HF cell S/N 15.

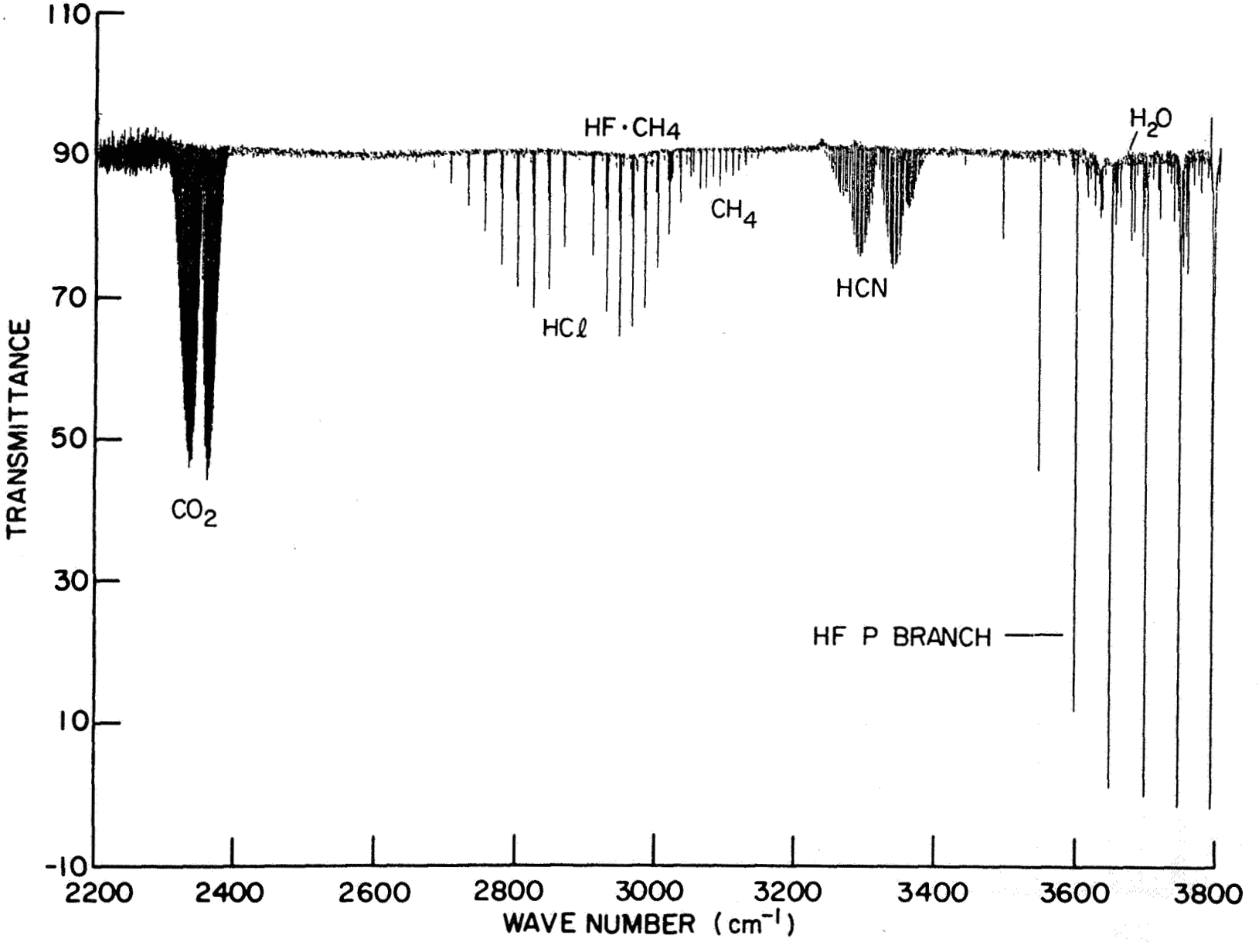

Figure 19.- Survey spectrum for HF cell S/N 16.

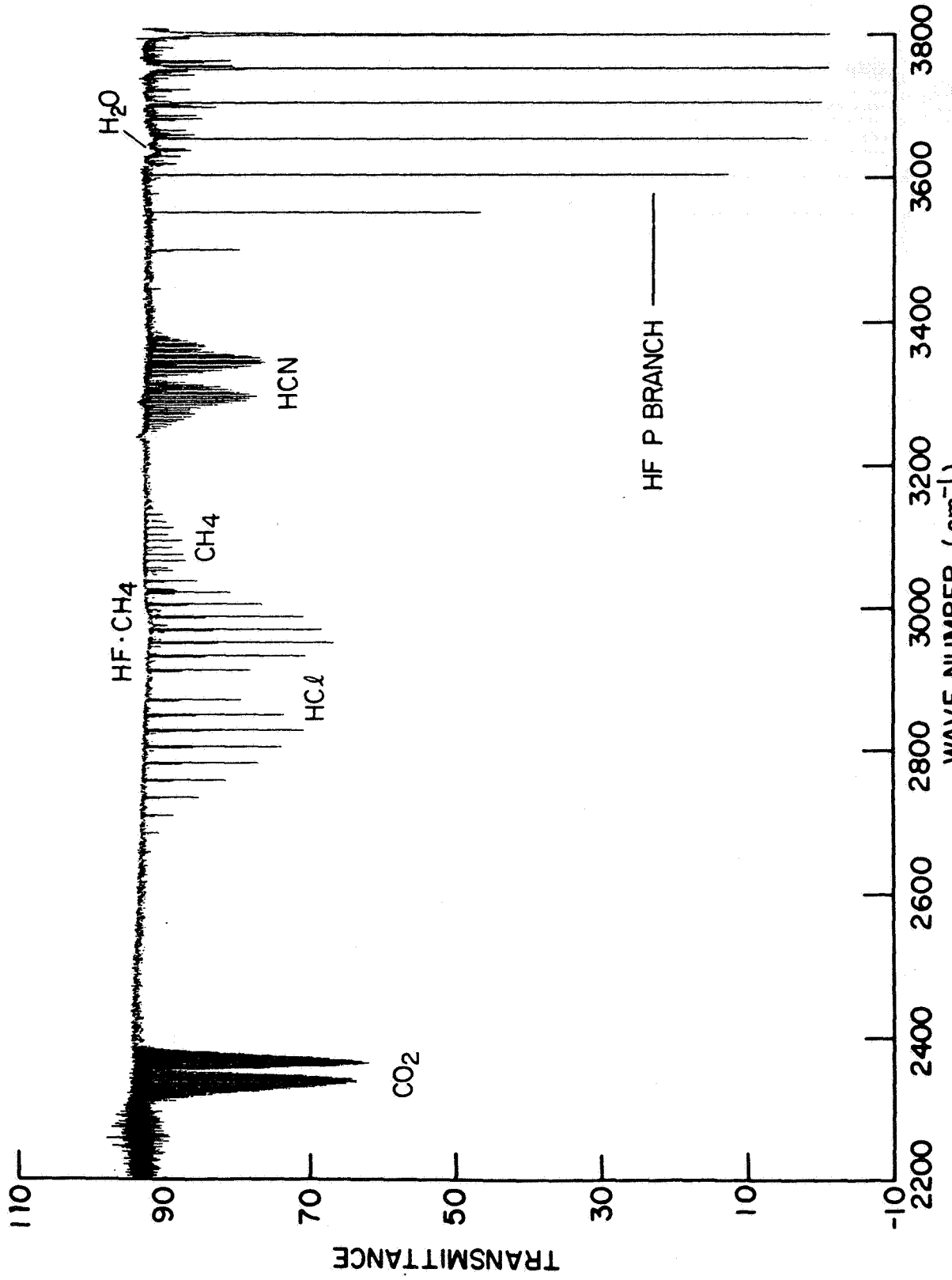

Figure 20.- Survey spectrum for HF cell S/N 17.

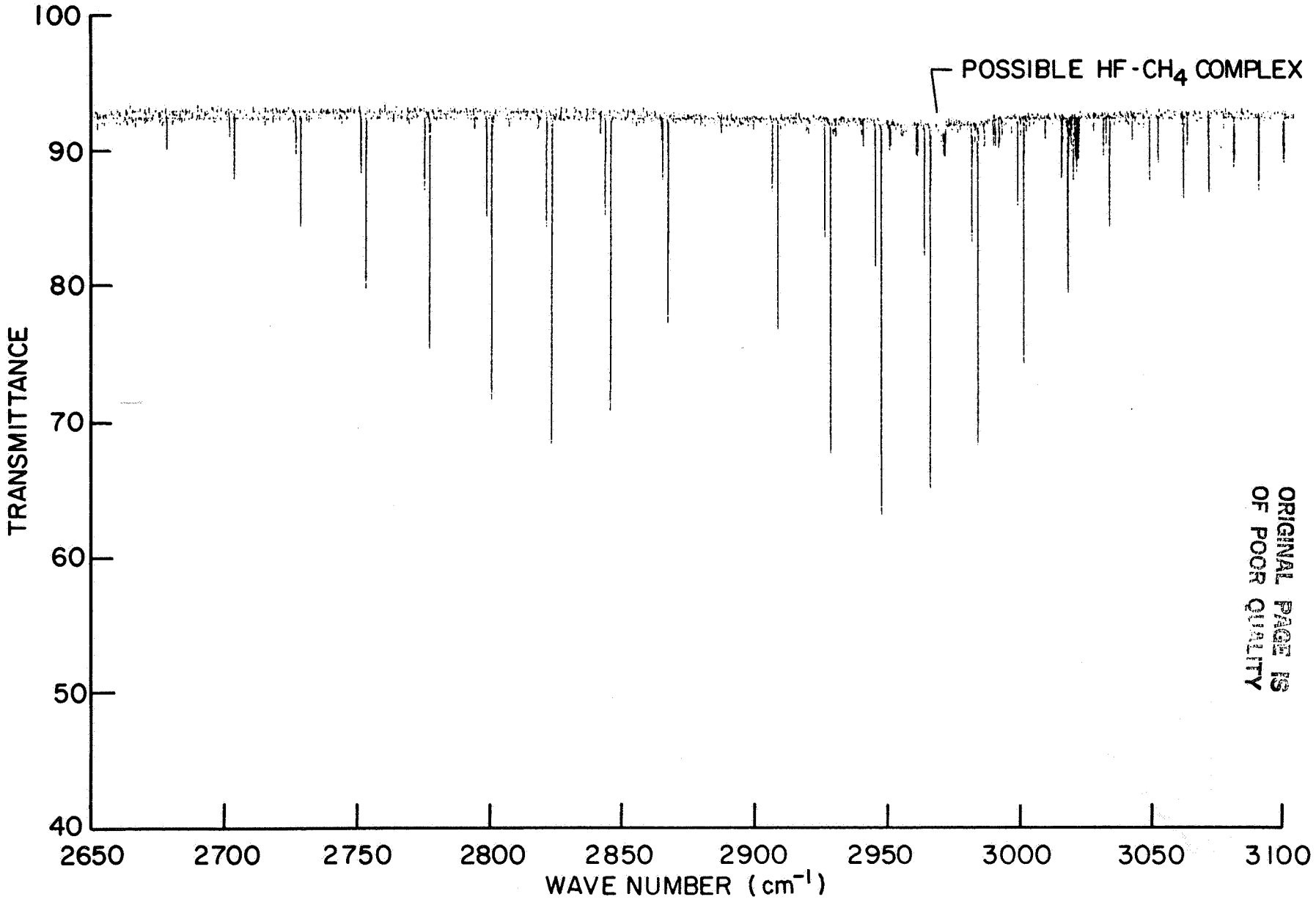

Figure 21.- HCl spectrum at ambient temperature in cell filled with HF: N_2 mixtures (HF cell S/N 16).

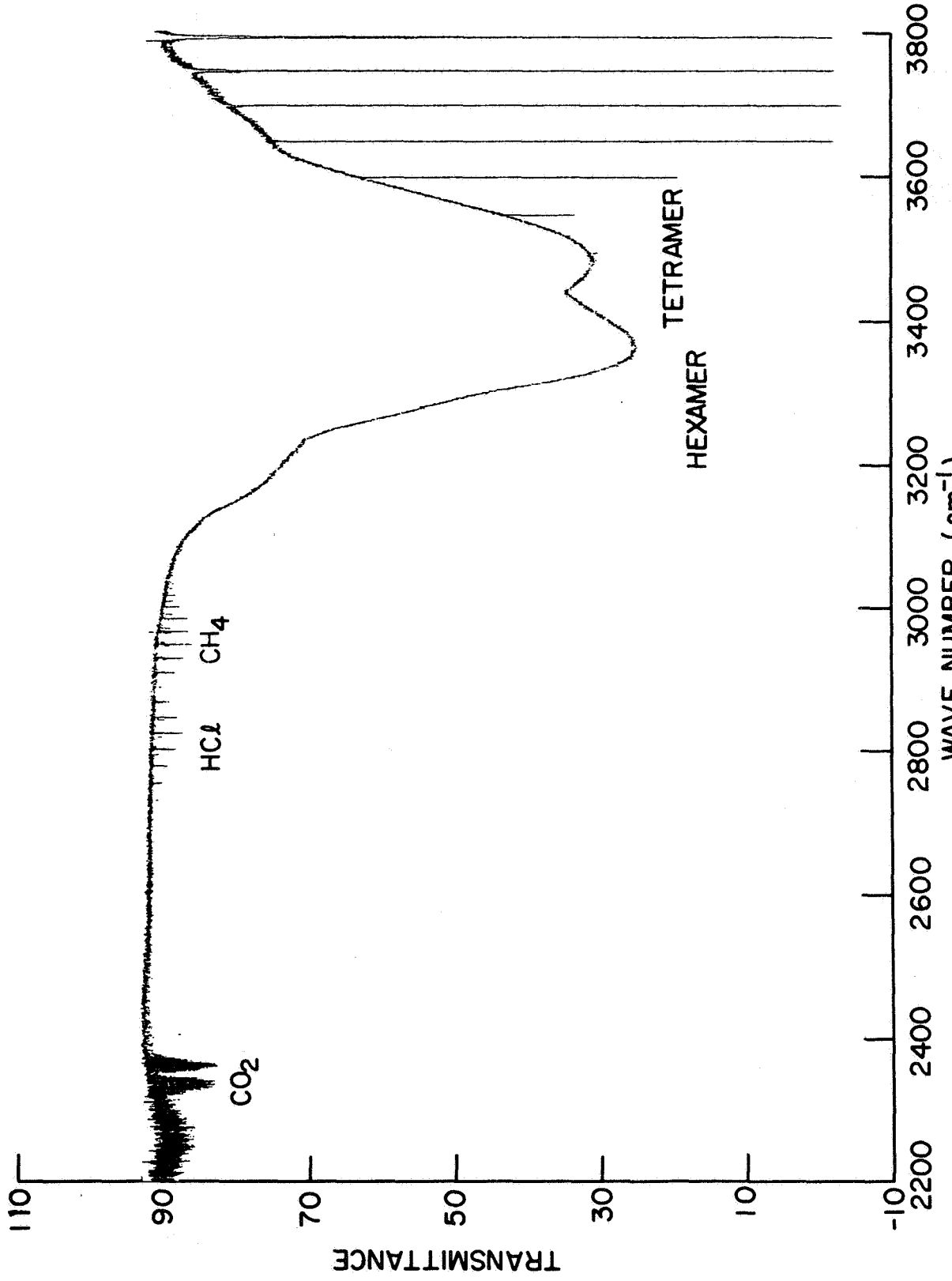

Figure 22.- Spectrum from reduced temperature (261 K) test of HF cell S/N 15.

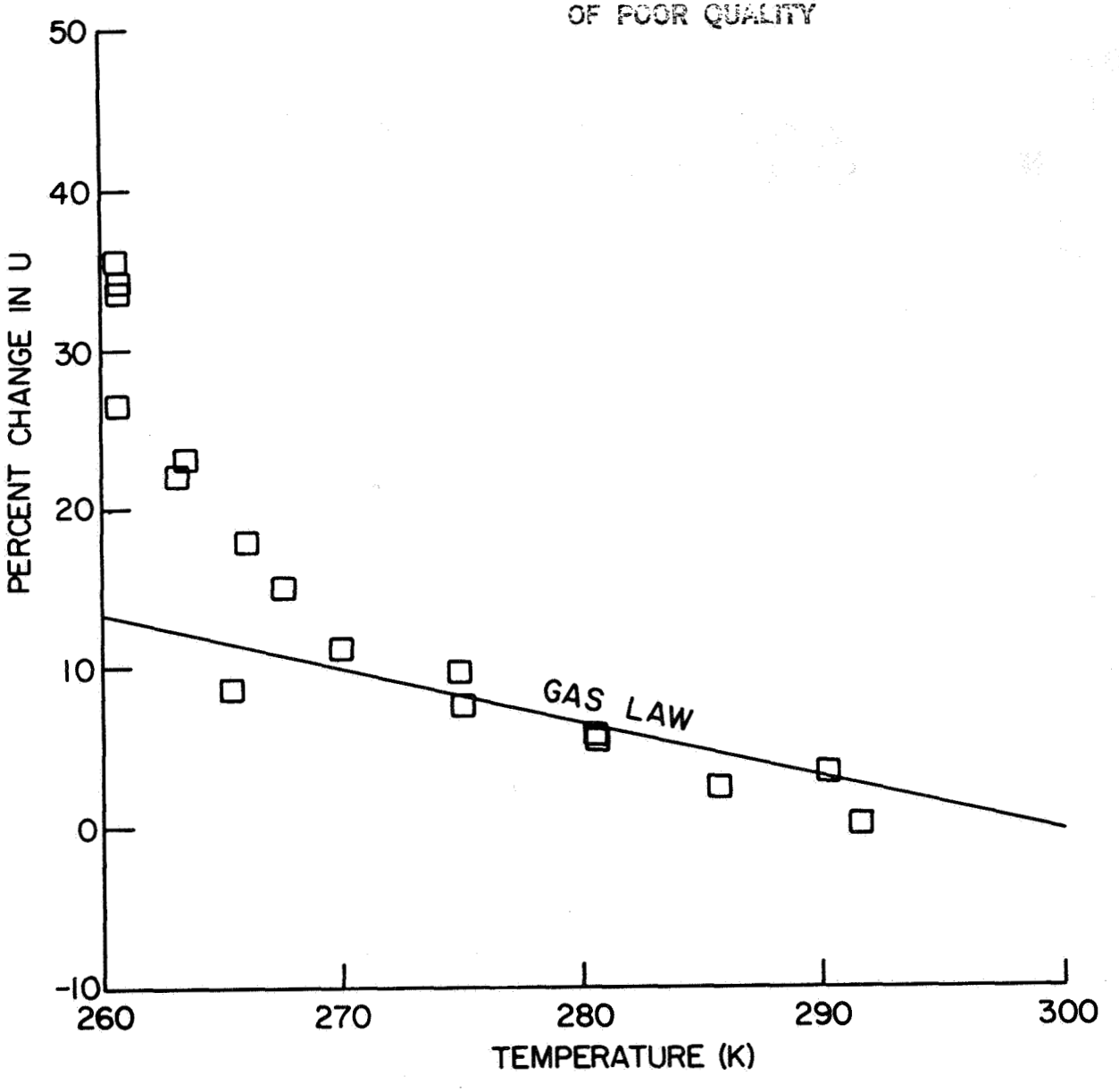

Figure 23.- Percent change in optical mass as function of temperature (gas loss due to polymer) for HF cell S/N 15.

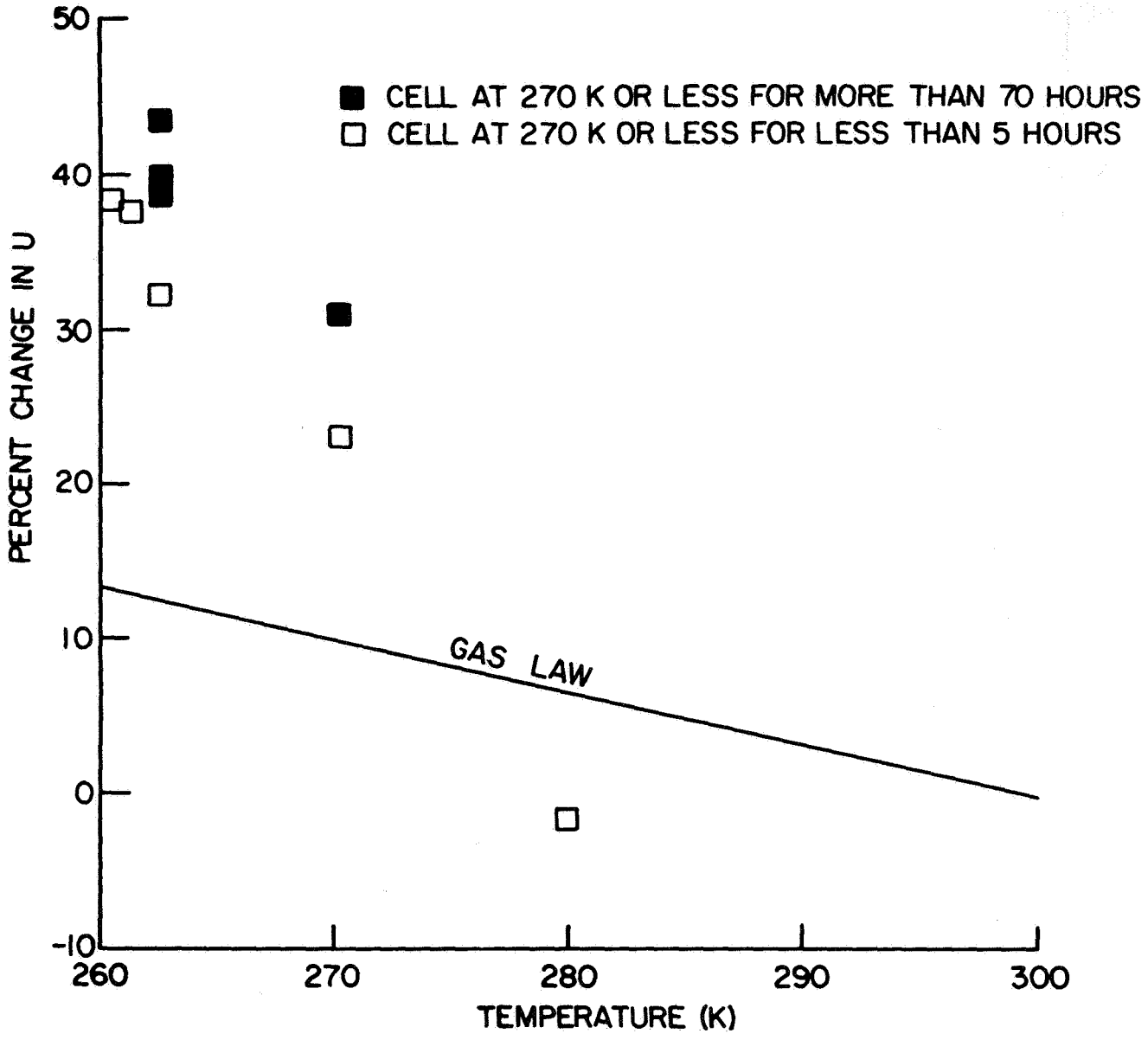

Figure 24.- Percent change in optical mass as function of temperature (gas loss due to polymer) for HF cell S/N 22.

1. Report No.	2. Government Accession No.	3. Recipient's Catalog No.
NASA TM-84640		

4. Title and Subtitle	5. Report Date
HALOGEN OCCULTATION EXPERIMENT (HALOE) GAS CELL LIFE TEST PROGRAM	August 1983
	6. Performing Organization Code 678-12-03-07

7. Author(s)	8. Performing Organization Report No.
Edward M. Sullivan, Robert E. Thompson, Gale A. Harvey, Jae H. Park, and D. J. Richardson	L-15581
	10. Work Unit No.

9. Performing Organization Name and Address	11. Contract or Grant No.
NASA Langley Research Center Hampton, VA 23665	

12. Sponsoring Agency Name and Address	13. Type of Report and Period Covered
National Aeronautics and Space Administration Washington, DC 20546	Technical Memorandum
	14. Sponsoring Agency Code

15. Supplementary Notes

Edward M. Sullivan, Gale A. Harvey, and Jae H. Park: Langley Research Center, Hampton, Virginia.
Robert E. Thompson and D. J. Richardson: Systems and Applied Sciences Corporation, Hampton, Virginia.

16. Abstract

The Halogen Occultation Experiment (HALOE) will use gas filter correlation radiometry to measure the atmospheric concentration profiles of HCl, HF, NO, and CH_4 from the Upper Atmosphere Research Satellite. The need to contain the gases for the gas filter measurements has resulted in the development of gas cells and the need for a life test program to demonstrate that the gas cells will perform their functions for extended periods (several years) of time. This report describes the tests in the life test program, the test apparatus used, and the analysis techniques developed. The report also presents data obtained during the first 14 months of the test program.

17. Key Words (Suggested by Author(s))	18. Distribution Statement
Halogen Occultation Experiment Spectral correlation Gas cells	Unclassified - Unlimited Subject Category 35

19. Security Classif. (of this report)	20. Security Classif. (of this page)	21. No. of Pages	22. Price
Unclassified	Unclassified	73	A04

For sale by the National Technical Information Service, Springfield, Virginia 22161

NASA-Langley, 1983